NOISE MEASURING APPARATUS

By

Teong Cheng Lim

A thesis submitted to the Faculty of Science
in partial fulfilment of the requirements for the degree of
Master of Science.

Department of Electrical Engineering,
Faculty of Pure and Applied Science,
The University of Ottawa,
Ottawa, Canada.

1964

TABLE OF CONTENTS

ABSTRACT

Noise measuring apparatus has been assembled, using the principle that the time average of two uncorrelated noise signals tends to zero over a long period. Application of this principle makes it possible to eliminate the effect of background noise of the amplifiers used in the measurements.

ACKNOWLEDGEMENTS

I wish to express my thanks to Prof. O. Celinski for suggesting the problem and for his guidance throughout the course of the research; to Mr. R. S. Richard for his help and encouragement in preparation of the thesis.

This research was made possible through financial support from the National Research Council grant No. A-871.

INTRODUCTION

The work was devoted to the completion of the correlation type noise measuring apparatus. This comprised two high gain amplifiers, a multiplier and auxiliary equipment. The work was concentrated on the multiplier (square-law type) and dealt mainly with the output drift. The causes of drift were investigated and reduced to a minimum. One of the major causes of the drift was traced to the power supplies and a large portion of work was devoted to them.

The results obtained for the multiplier were: an error not more than 1%, a bandwidth of about 1Mc, an input range from 600 mV to 5V peak to peak and an output drift on the order of 10mV in eight hours.

The noise measuring sensitivity of the equipment when used as a straight amplifier and noise detector, was such that the noise originating in a resistor of 1000 ohms at the input could be detected.

Chapter I reviews the existing theory on the behaviour of (i) current-voltage characteristic of p-n junction biased in the forward direction at high current densities and (ii) the noise generated within the junction.

Chapter II presents a construction of a working multiplier.

Chapter III describes the auxiliary stabilizer for - 250 volt tap.

Chapter IV gives the results of the noise measurements.

CHAPTER 1

P-N Junction at high current density*

The diffusion theory of current flow in p-n junctions due to Shockley (1949) accounts satisfactorily for most phenomena associated with the forward current flow at moderate biases and hence at low injection levels. Steady-state voltage-current characteristic, ratio of hole to electron-current, alternating current behaviour and transient response are a few examples of problems which can be treated quantitatively on the basis of this theory. Essentially, Shockley's theory is based on the following three assumptions:

(1) The space-charge giving rise to the transition from n-type to p-type band structure is well defined and bounded by two planes such as a and b in Fig. (1.1-1), where outside this region space-charge neutrality is preserved.

(2) The electron and hole carrier densities n and p on these planes are in quasi-thermal equilibrium with each other so that:

$$\frac{n_a}{n_b} = \frac{p_b}{p_a} = \exp\left(\frac{eVd}{KT}\right) = \exp \mathcal{V}_d \qquad (1.1\text{-}1)$$

where e denotes the magnitude of the electron charge, K Boltzmann's constant, T the absolute temperature and Vd the diffusion barrier height.

(3) The densities of the injected minority carriers on either side of the transition region are small in comparison with the respective majority carrier densities.

---

* When a large field is applied to a p-n junction, minority carriers are injected into the base region from the emitters. These injected carriers tend to create a space charge; therefore, majority carriers enters from the base lead to neutralise the charge causing an overall increase in carrier concentration. "High current densities" imply the condition when the concentration of the injected carriers becomes comparable to or greater than the impurity concentration.

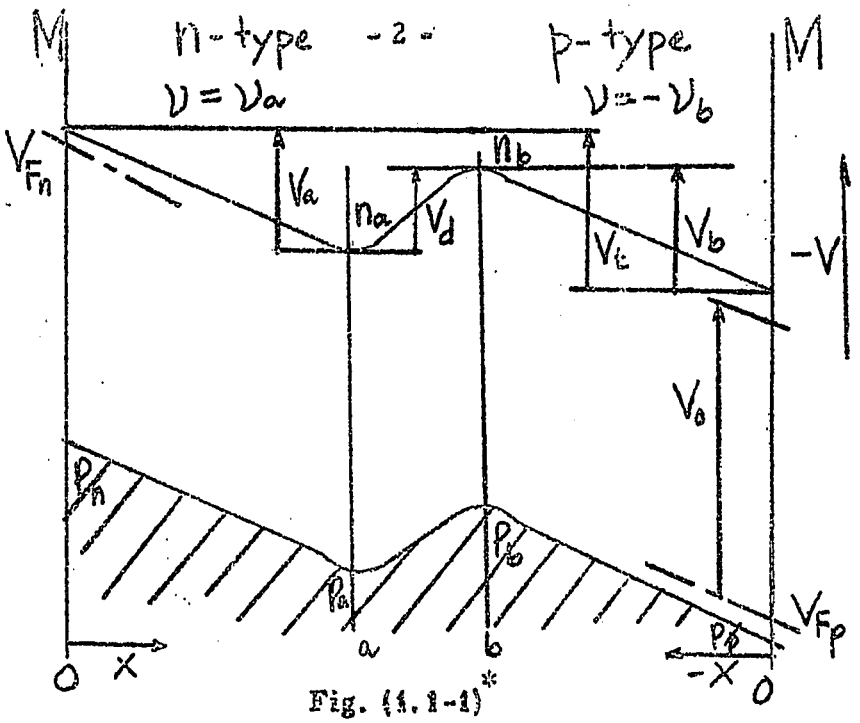

Fig. (1.1-1)*

n_a, n_b: The electron carrier densities at a, b in quasi-thermal equilibrium.

P_a, P_b: The hole carrier densities at a, b in quasi-thermal equilibrium.

n_n, P_p: The respective thermal equilibrium majority carrier densities.

n_p, P_n: The respective thermal equilibrium minority carrier densities.

V_d : Diffusion barrier height.

V_a : The potential drops across n regions.

V_b : The potential drops across p regions.

V_o : The barrier height in the absence of external bias.

V_t : Total electrostatic potential difference.

V_{F_p} : The Fermi-levels for holes.

V_{F_n} : The Fermi-levels for the electrons.

ν : Impurity density.

---

* Schockley, W. "Electrons and Holes in Semi-conductors".

One consequence of assumption (3) is that the electric field in the bulk n and p - regions is negligible as far as its effect on the minority carriers is concerned. Thus the minority carrier currents are purely diffusive. The second consequence is that n_a and p_b in equation (1.1-1) may be replaced by n_n and p_p, the respective thermal equilibrium majority carrier densities. This leads to the expressions

$$(\Delta p)_{x=a} = p_a - p_n = p_n [\exp(\mathcal{V}appl) - 1] \qquad (1.1\text{-}2)$$

$$(\Delta n)_{x=b} = n_b - n_p = n_p [\exp(\mathcal{V}appl) - 1] \qquad (1.1\text{-}3)$$

in which p_n and n_p are the thermal equilibrium densities of minority carriers in the n- and p- regions respectively, $\mathcal{V}appl = eVappl/KT$ and V appl is the externally applied potential difference. Since the currents are purely diffusive and proportional to Δp and Δn the voltage-current characteristic is obtained in the form:

$$I = I_e + I_n = I_s [\exp(\mathcal{V}appl) - 1] \qquad (1.1\text{-}4)$$

where I, I_e, I_n and I_s denote, respectively, the total current, its electron and hole components and the saturation current. In this approximation the whole externally applied potential difference appears at the junction since the potential drops in the bulk n - and p - regions are negligible.

The effects of carrier generation and recombination in the semi-conductor, especially at moderately high forward currents have been investigated (Fletcher 1957). The results may be summarized by the formula.

$$I \propto \exp(eV/nKT)$$

where n lies between 1 and 2, depending upon the type of recombination

and generation mechanism and the geometry of the junction.

The situation changes profoundly, however, on application of a sufficiently high forward bias so that the injected carrier densities are no longer small in comparison with the majority carrier densities, thus violating the assumption (3) above. In fact, the "minority" and "majority" carrier densities become eventually comparable in magnitude and the effect of electric field on both carrier species has to be considered. As a consequence, the carrier flow ceases to be purely diffusive. The conductivity is modulated to a considerable extent, the potential drops in the p- and n- regions become important and the voltage current relation given by equation (1.1-4) does not apply.

A strict solution of the problem requires the solution of a system of differential equations expressing the continuity conditions for currents and Poisson's law. For a one-dimensional case these may be written in the form:

$$I_e = b_o e(\mu_h nE + D_h \frac{dn}{dx}) \qquad (1.1\text{-}5)$$

$$I_h = e(\mu_h pE - D_h \frac{dp}{dx}) \qquad (1.1\text{-}6)$$

$$\frac{dE}{dx} = \frac{4\pi e}{K}(p-n+N_D^+-N_A^-) \qquad (1.1\text{-}7)$$

where K is the dielectric constant, e the magnitude of electronic charge, μ_h, D_h are the mobility and diffusion constant for holes, b_o μ_h is the electronic mobility, E is the electric field, N_D^+, N_A^- are the ionized donor and acceptor densities respectively. These equations should be supplemented, in the general case, by equations expressing div. I_e and div. I_h as a result of recombination, where a suitable model for the recombination process has to be chosen.

A complete solution of this problem has not yet been published and in any case, it is likely to be in a prohibitively complicated form, as may be seen from a number of papers by Russian authors which have appeared recently (Avak'yants, Murgyin, Sandles, Teshabayev and Yuroskiy 1963), (Yesina, Zotova and Nasledov 1963). The papers of Tolpygo and Zaslavskaya (1955), Tolpygo (1957) deal with the problem of diffusion in the region of high injection, taking into account various models for recombination. The formulae are difficult to interpret in terms of V-I characteristics, but Kosenko (1957) attributes to them the form:

$$I \propto (V - V_0)^{\frac{3}{2}} \qquad (1.1\text{-}8)$$

where Vo is the diffusion potential.

The case of a completely symmetric junction having equal mobilities, diffusion lengths, widths and impurity densities of both regions has been treated by Herlet (1956). The result is that the potential drop in the diffusion regions is proportional to $I^{\frac{1}{2}}$. This particular treatment is not applicable, however, to asymmetric junctions which are most important from the point of view of practical applications. But the Russian authors (Avak'yants, Murgyin, Sandler, Teshabayev and Yurovskiy (1962)) have attempted solving the asymmetric junction problems by assuming new boundaries conditions for minority carriers at the boundaries of a base with a space-charge region with Boltzmann distribution. Furthermore, there is very little published experimental evidence relating to the behaviour of p-n junction in the region of very high current densities, where the exponential relation no longer applies.

Regarding the noise in p-n junctions, good agreement has been found between experimental and calculated values at low current density by Guggenbuehl and Strutt (1957) and Van de Ziel (1959).

In these experiments, Van der Ziel's noise equivalent circuit used to obtain the calculated results is shown in Fig. 1.1-2.

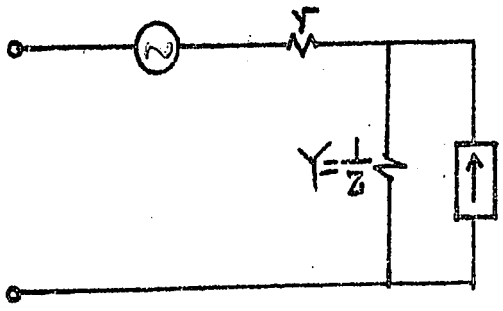

Fig. (1.1-2)

This equivalent circuit is a noise-free junction of admittance Y in parallel with a noise current generator of mean square value

$$\overline{i^2} = [4kTRe(Y) - 2eI]\,df \qquad (1.1\text{-}9)$$

where Re(Y) is the real part of the junction admittance.

The above equation was derived on the assumptions[13]:

1) that the noise is attributed to a series of random and independent crossings of the junction by current carries and

2) that traps present in the space charge region have no effect on diffusion. Thermal noise is due to the contact resistance and the extrinsic base resistance is excluded from equation (1.1-9) but is represented by a resistor r in Fig. (1.1-2) equal to the contact resistance plus the extrinsic base resistance showing full Nyquist noise.

At high current densities, both the minority and majority carries densities increase above their equilibrium values i.e. above the concentration of carriers found in the semi-conductor material in the absence of an external field. Under these conditions, it was found[14] that equation (1.1-9) failed to predict the noise properties.

Two postulates were (Appendix 6) put forward by A. Van der Ziel and W. Guggenbuehl and M.J.O. Strutt. Up to now neither of these postulates has been verified experimentally nor proved theoretically.

B. Schneider and M.J.O. Strutt (1960) have measured the noise in p-n junctions at high current densities assuming the above effects to be trivial. They calculated the junction noise by applying a new equivalent circuit as shown in Fig. (1.1-3)

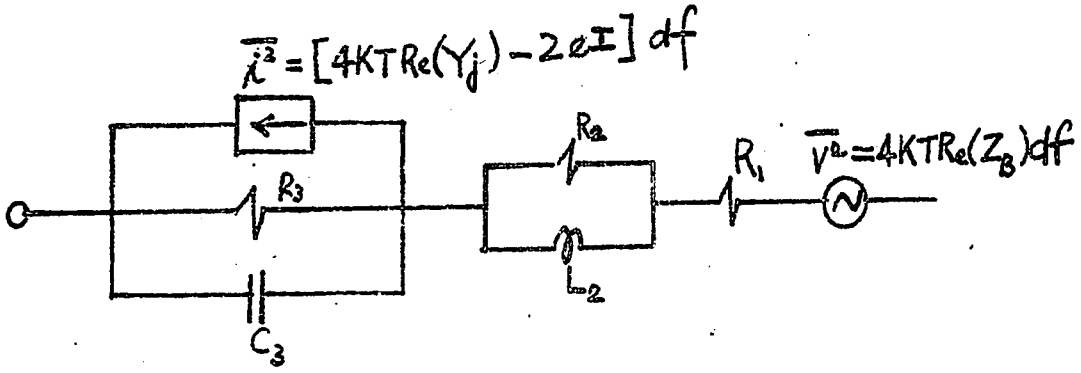

Fig. (1.1-3).

where Z_B is the impedance of the semiconductor material outside the space charge regions and its noise is given by

$$\overline{V_n^2} = 4kTRe(Z_B)\ df. \qquad (1.1\text{-}10)$$

However, H.F. Mataré (1958) has suggested a different expression of the noise current generator of fig. (1.1-2) under high current density and is given by

$$\overline{i^2} = [4kTRe(Y) + 2eI]\ df \qquad (1.1\text{-}11)$$

W.R. Samaroo (1961) has shown that the above equation of Mataré holds for temperature $4.2^{\circ}k$ and $80^{\circ}k$. and Eq. (1.1-9) is good for room temperature.

Very little work seems to have been done on the measurements of noise in p-n junction at high current densities. One of the main reasons for this seems to be the difficulty of making these measurements with reasonable accuracy because of the low level of the noise. These difficulties therefore present a challenge and the remainder of this thesis describes an attempt to meet this challenge.

CHAPTER 2

The Multiplier

2.1 Purpose and Specifications:

The project is a continuation of the work of W. Samaroo (1961), which was concerned with the measurements of current noise in p-n junction at low temperatures. The sensitivity of the equipment which was sufficiently high for the measurements on p-n junction biased in the reverse direction was not high enough to measure the noise generated in a junction biased in the forward direction. This was particularly inadequate for noise measurements at high current densities when the resistance of the p-n junction was only a few ohms*.

It has therefore been decided to try a different approach to noise measurements. The chosen method makes use of the fact that if two uncorrelated noise signals of zero mean value are multiplied together their product is zero on the average. This makes it possible,

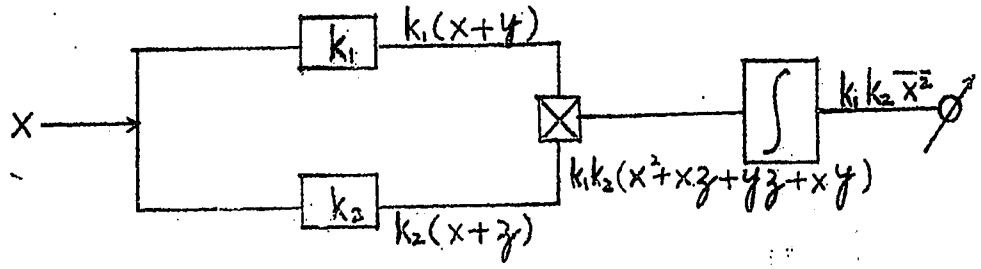

Fig. 2.1-1.

---

* In p-n junction, the flow of current is

$$I = I_o\left(e^{\frac{eV}{KT}} - 1\right)$$

where I_o is the reverse saturation current and V is the voltage applied to the junction. Differentiating with respect to V gives

$$\frac{dI}{dV} = \frac{e}{KT} I_o e^{\frac{eV}{KT}} = \frac{e}{KT}(I + I_o)$$

$$= \frac{e}{KT} I \text{ for } I \gg I_o$$

$$\therefore R = \frac{dV}{dI} = \frac{KT}{eI}$$

in principle, to eliminate the unwanted background noise of the amplifiers used in the measurements. An explanation of this method is shown in a simplified block diagram in Fig. (2.1-1). In this diagram x is the noise coming from the p-n junction. This signal is amplified in two channels k_1 and k_2 which add the unavoidable background noise y and z. The outputs of the amplifiers containing both wanted and unwanted noise are multiplied together in the multiplier X and then averaged. This averaging process eliminates, in principle, all unwanted signals leaving only the mean square value of the noise coming from the junction.

Thus

$$\lim_{T\to\infty} \frac{1}{T}\int_0^T [\, x^2 + xz + xy + yz \,]\, dt = \overline{x^2}$$

provided that the average of each of x, y, z, signals is separately zero and that there is no correlation between either pair of these signals.

This noise measuring method requires two amplifiers, a multiplier, and an integrator.

It is desirable that the multiplier has the following characteristics.

1) Accuracy:

To measure noise power with an accuracy of about 1% the multiplier error must be of the same order --- i.e. 1% or less.

2) Input:

Assuming the use of the presently available amplifers (RCA Communication Receivers Model 150A) which are capable of delivering about 30V peak-to-peak into a 600Ω load the multiplier should have a signal handling capacity on the same order and an input impedance of 600Ω or higher.

3) Output:

It would be desirable to have an average output voltage of not less than 2.5V at an impedance of a few hundred ohms, say. This would make it possible to use a moving coil meter as an output monitor.

4) Stability:

The dynamic range of the multiplier input is about 4V peak-to-peak. Assuming that a noise signal of 4V peak-to-peak has an average value of about 200mV we can obtain an output on the order of 2mV. The stability of the multiplier should therefore be such as to make it possible to measure this voltage since the time constant of the integrator is about 20 sec. and the measurement error should not exceed 1% therefore the drift in the multiplier output should be not greater than 2mV/20 sec = 0.01 or about 1μV per second.

5) The multiplier must not be restricted in the sign of the inputs i.e. it has to be a four-quadrant type.

6) The amplifier used here (communication receiver RCA Model 150A) has a maximum bandwidth of 6 KC and therefore, the multiplier should have a bandwidth of not less than 6KC.

The integrator is intimately linked with the multiplier in this type of measurements and its specifications are given here.

1) For a bandwidth of 6 KC and an error of 0.5% the time constant should be at least 5 seconds. (see eq. 2.3-8). As a starting point, we are adopting two time constants of 10 and 20 sec.

2) Because of the direct relation between the integrator and the multiplier the error and the stability for the former should not exceed the corresponding values for the latter i.e. 1% and 1μV per second respectively.

2.2 Description and Construction.

The square-law multiplier which is described in this thesis was adopted from the work of K.D.J. Grosvenor (1959) and it satisfies only some of the specifications mentioned above.

The reasonsfor adopting this particular multiplier in spite of its inadequacy were a) its accuracy (claimed 1%), b) its bandwidth (claimed 2 mC) and c) its availability. The work on this multiplier was started by I.H. Rimawi in 1962 and completed by the writer in 1964.

Definition

"A square-law multiplier is a nonlinear multiplier in which the sum and the difference of the variables are squared and then subtracted leaving an output that is proportional to the product of the two variables" (Rimawi 1963). A block diagram of such multiplier is shown in Fig. 2.2-1.

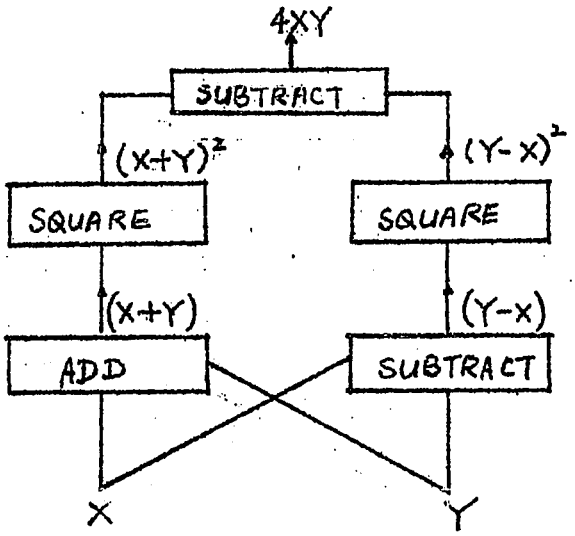

Fig. 2.2-1.

The square-law multiplier used in this project was a minor modification of Fig. 2.2-1. The principle of operation was the same.

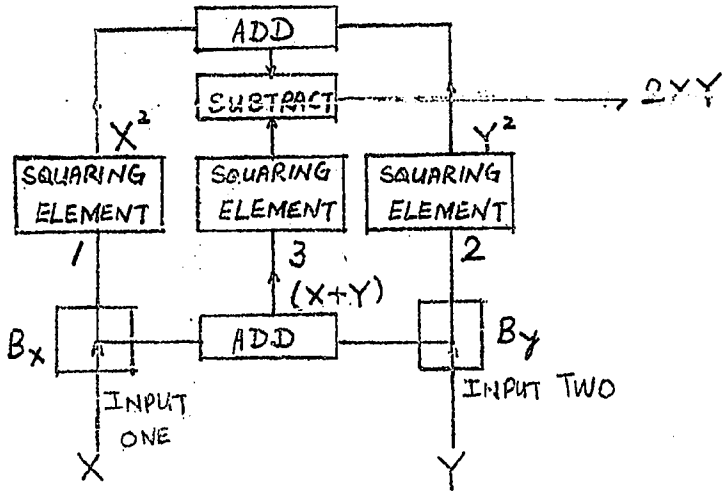

Fig. 2.2-2.

Fig. (2.2-2) shows this modified multiplier. The input signals are applied separately through buffers B_x and B_y to the squaring elements 1 and 2 and the sum of the inputs is applied to the squaring element 3. The output of squaring element 3 is then subtracted from the summed outputs of squaring element 1 and this leaves the final product proportional to XY.

The above description assumes the existence of an ideal squaring element. Since such elements strictly speaking are non-existent, it is therefore necessary to use a more general nonlinear element of the type

$$I = A + BV + CV^2 + \ldots . \qquad (2.2\text{-}1)$$

where V is the signal voltage and A, B and C are constants.

By suitable circuit arrangement, it is possible to eliminate the constants A and B with an arbitrary accuracy. This gives us the required squaring effect from such an element and is shown in Fig. 2.2-3.

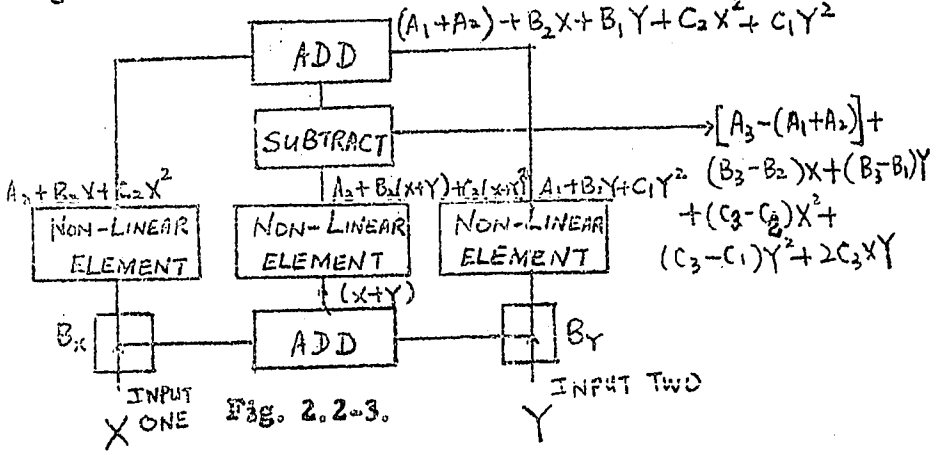

Fig. 2.2-3.

Since the output of the multiplier

$$V = [A - (A_1 + A_2)] + (B_3 - B_2) X + (B_3 - B_1) Y + (C_3 - C_2)$$

$$X^2 + (C_3 - C_1) Y^2 + 2C_3 X Y \qquad (2.2\text{-}2)$$

contains factors made of differences between the coefficients A, B and C, therefore, by making all three non-linear elements identical we can, in principle, eliminate all terms except the product term $2C_3XY$. This gives us the result required of the multiplier.

While the elimination of constants A, B and C can be effected with an arbitrary accuracy, and therefore the multiplier accuracy can be arbitrarily high, there are factors contributing to the error, which cannot be eliminated. These result in an error of value of about 1%. One of those factors is the existence of higher terms in the assumed transfer characteristic of the nonlinear element. If we assume the presence of the third order term.

$$I = A + BV + CV^2 + DV^3$$

the error due to D is on the order of 0.5% (see Appendix 3).

The descriptions below are referred to Fig. 2.4-10.

"Nonlinear elements"

The multiplier requires a nonlinear element of the square law type. Tubes 5670 which are used here have a region of operation in which the transfer characteristic (2.2-3) follow this law (see Fig. 2.2-4).

This transfer characteristic can be described by the current voltage relation

$$I = A + BV + CV^2 \qquad (2.2\text{-}3)$$

where I is the plate current, V is the grid voltage and A, B and C are constants.

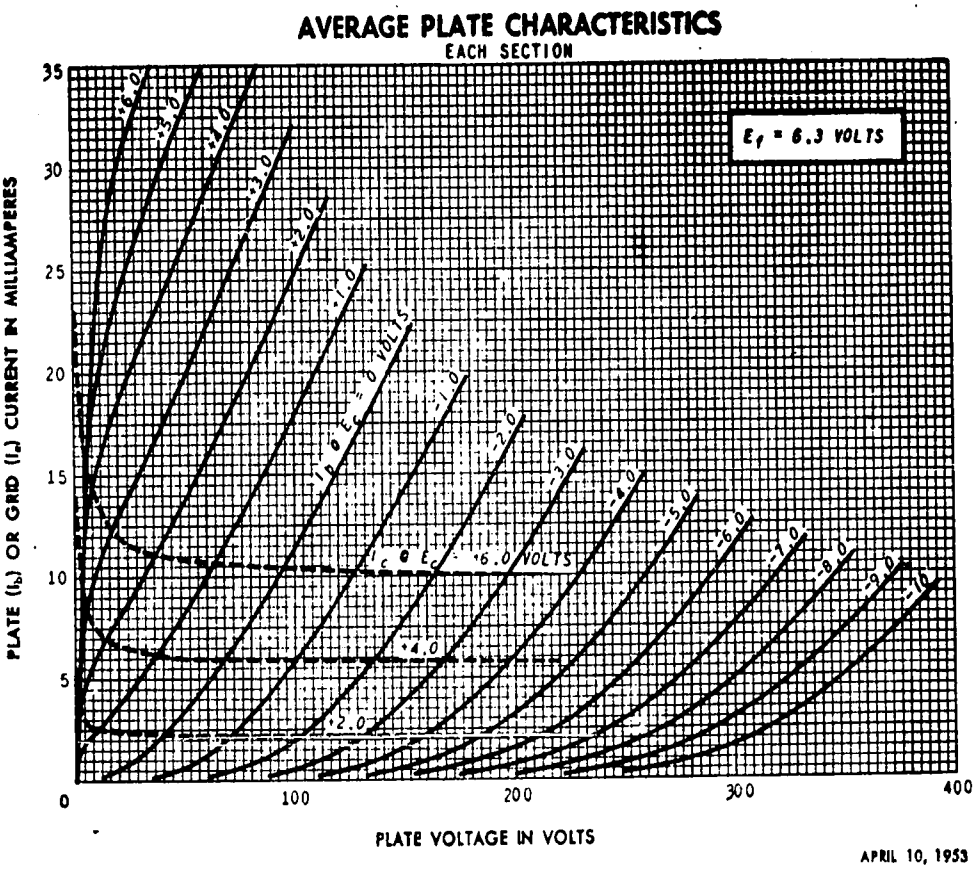
AVERAGE PLATE CHARACTERISTICS
EACH SECTION
E_f = 6.3 VOLTS
PLATE (I_b) OR GRID (I_c) CURRENT IN MILLIAMPERES
PLATE VOLTAGE IN VOLTS
APRIL 10, 1953

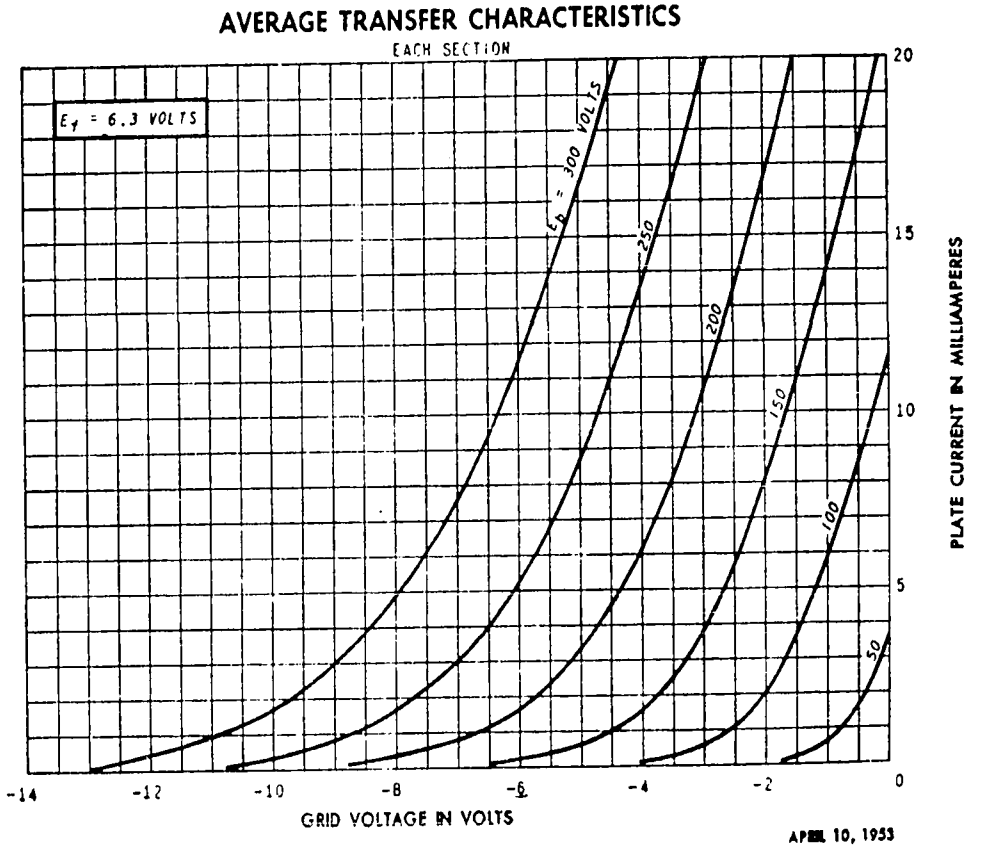
AVERAGE TRANSFER CHARACTERISTICS
EACH SECTION
E_f = 6.3 VOLTS
E_b = 300 VOLTS
PLATE CURRENT IN MILLIAMPERES
GRID VOLTAGE IN VOLTS
APRIL 10, 1953

Fig. 2.2-4

This relation holds only within a certain region of grid voltages in the vicinity of $-1.5 \gtrless V \gtrless -3.5V$. For a signal which has a zero mean value, such as noise, the tube requires a bias of a about $-2.5V$ to keep it within the required operating region.

In this particular circuit a current sink (tubes V_{12} and V_{22}) is used for this purpose. For proper operation of the multiplier all three nonlinear elements should be identical. Since this implies the equality of the corresponding coefficients ABC for the three tubes (see Fig. 2.2-3) therefore, it is necessary to provide facilities for adjustment of these coefficients.

The adjustment of the coefficient A (the d-c component of the plate current) is a trivial one (see the "output stage"). The coefficient B (the transconductance of the tube) can be adjusted by changing the tube bias. The coefficient C (the rate of change of transconductance) can be adjusted by changing the plate voltage of the tube.

Changing the plate voltage of this tube, without significantly affecting other parameters, can be done by using a cascode* configuration. This configuration has additional advantages of providing a good isolation between the input grid and the output plate and also of presenting a high effective plate impedance. This is important in the add operation. (Grosvenor, 1959).

Buffer stages: (V_{11}, V_{21})

These stages isolate electrically the multiplier from the signal sources. In order to minimise any variations in this stage a large amount of negative feedback is used. The voltage gain was arbitrarily fixed at 0.50.

---

* A cascode stage consists of a grounded grid triode in cascade with a grounded cathode triode. The upper tube plate characteristics (plate voltage versus plate current curves for constant grid voltage of the lower tube) resemble those of a high resistance pentode.

The Adder: (V_3)

This circuit is a simple resistive adder where currents due to signals X and Y are combined in the common plate resistor R_{25}. The function of the tubes is to transform signal voltage sources into current sources. Any errors in this circuit are due to the nonlinearities of the tubes and to their finite resistance.

To minimise these errors and any variation in this circuit a large amount of negative feedback is used similarly as in the buffer stages.

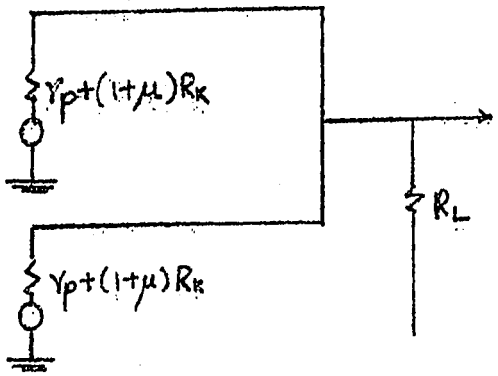

Output stage:

The cathode follower isolates electrically the multiplier from the integrator and provides a low impedance source of about 300 ohms to the latter. R_{33} and R_{34} together with the plate loads of V_4, V_5 and V_6 form potential dividers to bring the plate voltage of all these tubes to about - 6V. This value brings the cathode follower outputs close to the ground potential. Since it is convenient to have this potential exactly at ground level a fine adjustments of these voltages is provided by means of variable cathode loads R_{33} and R_{34}. Thus it is possible to bring the two output voltages to the ground potential in the absence of signal. This equalization of the two quiescent output voltages makes, in effect, the A constants of the nonlinear elements equal.

Integrators:

A simple RC integrating network is used at both outputs (R = 5, 25 and 50 kΩ, C = 400μf) The time constant of these networks is variable in three steps; 2, 10 and 20 seconds. The difference between the two outputs is measured across the output terminals 0_1 and 0_2, (see Fig. 2.2-5).

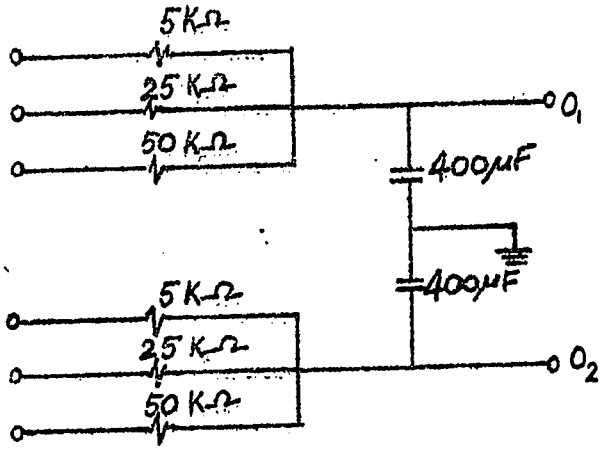

Fig. 2.2-5.

Design Consideration

2.3 Introductory remarks

Since this multiplier was adopted from an existing design, a number of features was adopted without questioning. These were the choice of tubes, supply voltages, stage gains etc. No attempt was made to improve the design but only to adapt it for the particular purpose for which it was intended in this project. The details of modifications are given by Rizzawi (1963). In the paragraphs that follow, some attention is given to the design considerations which are necessary for the construction of a working model.

The sequence of the description is as follows. The most important and critical part of the multiplier is the nonlinear element and therefore it is described first. The current sink is used to establish the correct working point for the nonlinear element and therefore comes second. Next follow the input and output buffers whose only function is to separate the sources and loads from the multiplier. The integrator design is included for the sake of completeness.

All the descriptions below are refegred to Fig. 2.4-10.

Cascode stages:

A square-law multiplier, as its name implies, requires an element having a square-law input-output characteristic. The cascode stages used here have the following current voltage transfer characteristic

$$i = A + BV + CV^2 \qquad (2.3\text{-}1)$$

where terms of the higher order have been neglected, i is the plate current and V is the grid voltage and therefore this type of current voltage transfer characteristic implies that A is the dc component of the plate current, $B = \frac{di}{dV}$ i.e. the transconductance of the tube in the absence of signal, $C = \frac{1}{2}\frac{d^2i}{dV^2} = \frac{1}{2}\frac{dg_m}{dV}$ = rate of change of transconductance of the tube.

It has already been pointed out (see section 2.2-1) that it is necessary to have the constants B and C identical for all three tubes. These constants can be made respectively equal by adjusting the plate voltage and grid bias on the tubes.

In order to effectively vary the plate voltage without changing the plate load, cascode stages have been used. (see Fig. 2.3-1).

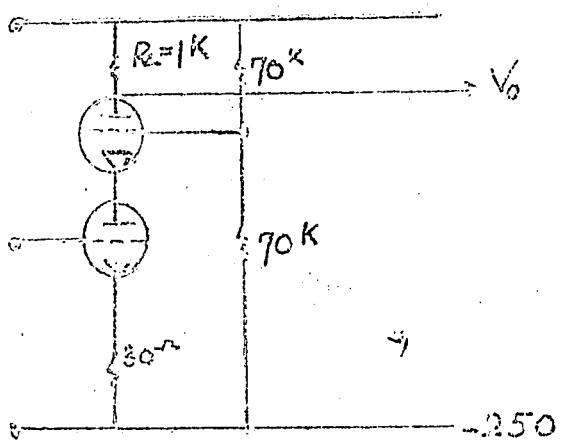

Fig. 2.3-1

The pre-setting of the grid voltage of the upper triode has an effect similar to that achieved when the plate voltage of a single triode is pre-set.

The cascode stages provide an isolation between the input grid and the output plate because of the shielding effect of the grid in the upper tube. This shielding is similar to that in a pentode. An additional advantage is the high effective plate impedance (about 240kΩ) which is desirable in the add circuit because of the otherwise undesirable shunting effect.

The tube 5670 has been chosen on the experimental basis since it has been found that this tube with a 30 ohms cathode feedback resistor gives a good approximation to the desired law (Eq. 2.3-1) (Grosvenor 1959). This is shown by the curves in Fig. 2.3-2 where the values for $R_k = 30\Omega$ give the best linearity of G_m with grid bias voltage

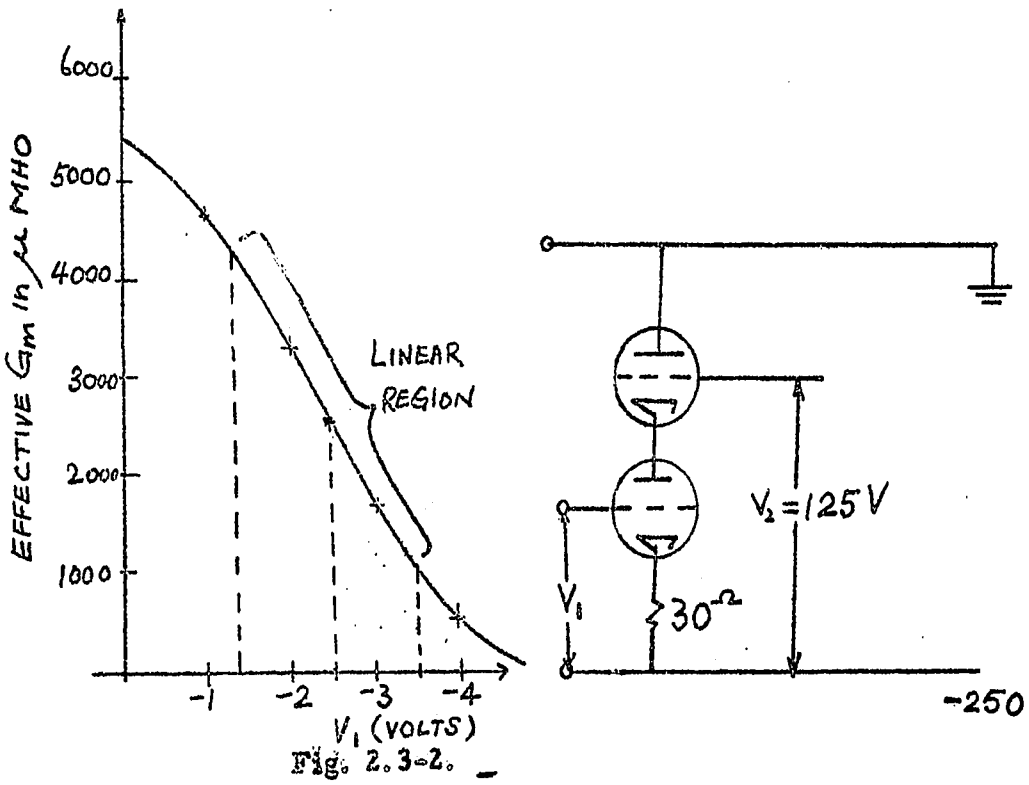

Fig. 2.3-2.

This figure also shows that the most suitable working point for a signal having a zero mean value is about - 2.5 V.

To make the G_m (transconductance of the tube) of different tubes equal, the plate voltage of the nonlinear element of the lower triode in the cascode stages is varied. This introduces another variable factor that has to be taken into account in establishing the most suitable working point. We have to meet two requirements here. The absolute value of G_m at the working point and its rate of change has to be the same for all three tubes.

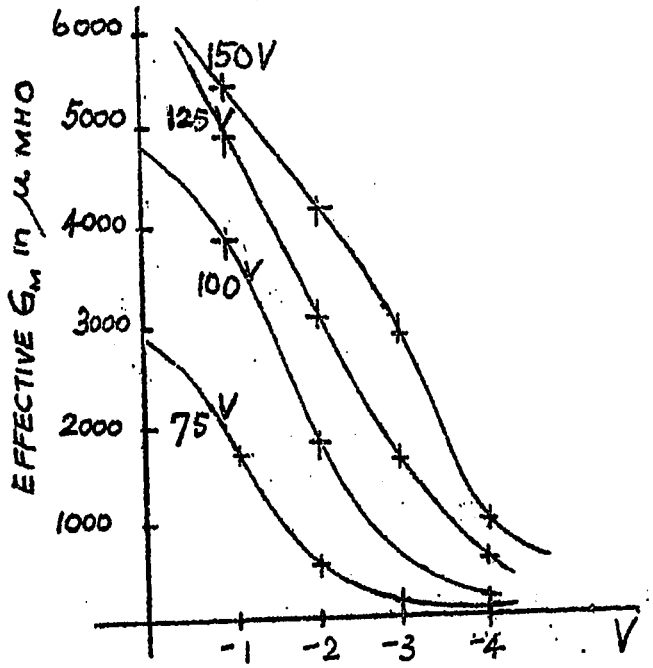

Fig. 2.3-3.

The curve for V_2 = 125V is the most linear over the widest range of grid voltages.

Fig. 2.3-2 and 2.3-3 show that this can actually be done. The value of G_m is very easily varied by the grid bias and therefore adjusted to the same value for all three tubes, and the slope of the G_m curve is adjustable by varying the plate voltage. The two adjustments are largely independent in a cascode configuration.

Current sink:

In the following description all voltages will be referred to the -250 volt level. The bias required for the lower grid of the cascode stage is about -2.5V. The plate voltage in the buffer stage is about -6 volts

on the average. A current is fed through a fixed resistance R_{21} so as to make the buffer stage plate close to the zero potential. The presence of this resistance does not affect the gain of the buffer stage since it is fixed and forms a part of the load. The buffer plate voltage is brought down again, this time to the required value of -2.5V by using the tube V_{12} as a current sink.

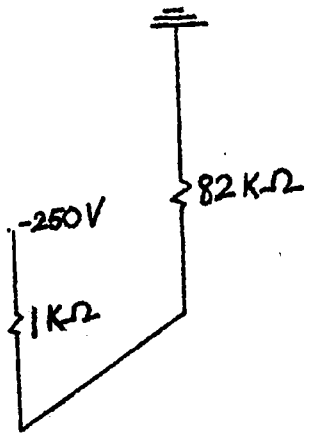

Fig. 2.3-4.

As a current sink, this tube (V_{12}) should have a negligible loading effect on V_{11}. The shunting resistance R_s of the current sink (V_{12}) is

$$R_s = r_p + (1+\mu)R_k \qquad (2.3\text{-}2)$$

for the limiting values of $7 \leq r_p \leq 12k\Omega$ and $30 \leq \mu \leq 60$

we get $22.5k\Omega \leq R_s \leq 195k\Omega$.

Input Buffer stages:

This is a grounded cathode amplifier with cathode degeneration. Its gain is given by

$$K = \frac{\mu R_3}{r_p + R_3 + R_k(1+\mu)} \qquad (2.3\text{-}3)$$

which is arbitrarily chosen to be 0.5. This allows for a large amount of feedback in the cathode thus making this stage stable and relatively insensitive to tube parameter changes and also it reduces the effect of non-linearities. In order to adjust the gain to this value, the cathode resistance R_k is made variable. The load resistance R_L is 1kΩ. By assuming the tube parameters to be within the limits $30 \leq \mu \leq 60$ and $7 \leq r_p \leq 12k\Omega$, we obtain the range of variation for R_k from

$$R_k = \frac{\mu R_3 - k(r_p + R_3)}{k(1 + \mu)} \qquad (2.3\text{-}4)$$

which for the numerical values above gives $1.6 \leq R_k \leq 1.9$. To satisfy this condition resistances were chosen as shown in the circuit diagram of this stage in Fig. (2.3-5)

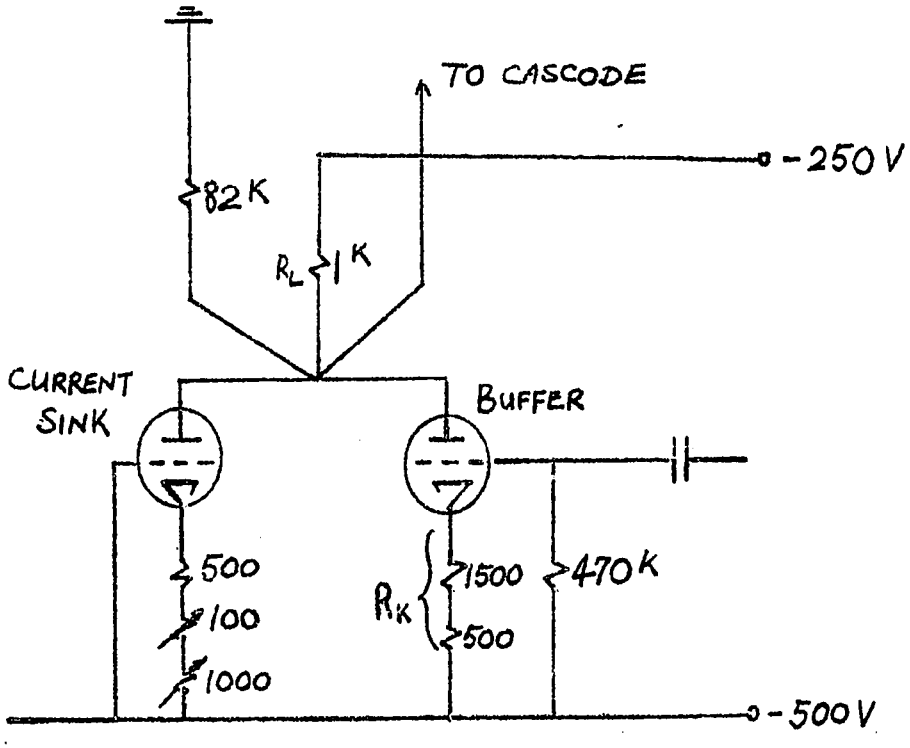

Fig. 2.3-5

Output Buffers:

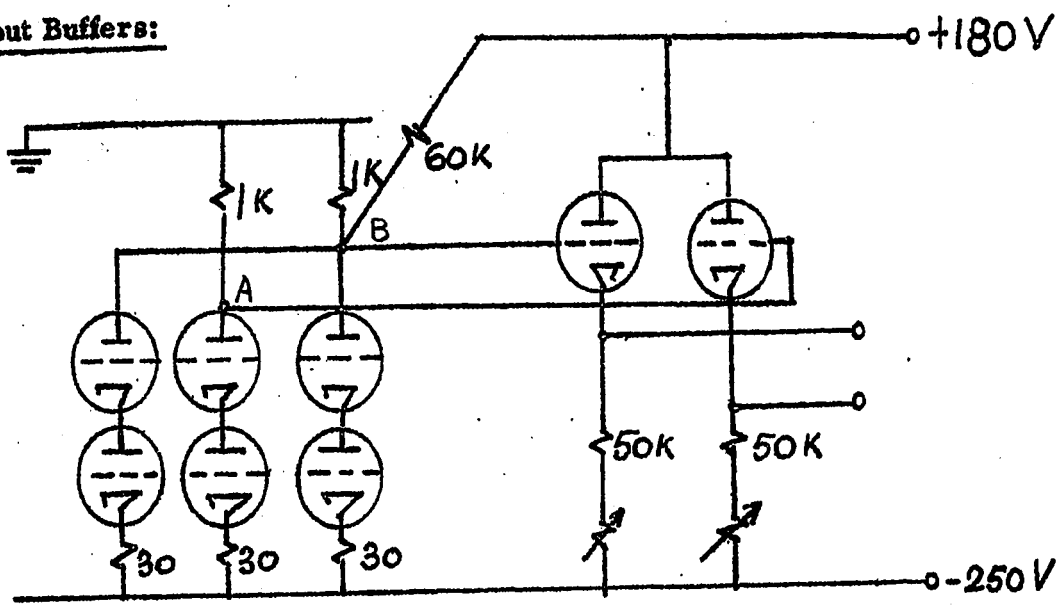

Fig. 2.3-6.

The two multiplier outputs A and B (see Fig. 2.3-6) are at voltage levels of about -6 and -3 volts respectively. Because of the necessity of performing a subtraction operation on these outputs it is necessary to bring these voltages to the same level in the absence of signal. This is equivalent to making A-coefficients in eq. 2.2-2 equal to zero.

In addition to this we have to separate the integrators from the multiplier and provide a low impedance source for the latter.

Cathode followers are used to satisfy both of these requirements. The second requirement is easily met by using relatively high G_m tubes (12AT7) which, at the working point used, provide an estimated output impedance of a few kiloohms.

In order to bring the quiescent output of the cathode followers to the same level two devices are used. First, the level of the A output is raised to approximately that of B by feeding a current of about 3ma from the +180V source (R43). The fine adjustment of these

two voltages is accomplished by varying the cathode resistors in the cathode followers. This has the effect of changing the potential between the grid and cathode of the tube. In this case the quiescent grid potential remains unchanged and the cathode potential varies. Thus a fine control is provided of the output level which has no effect on the multiplier. This makes it possible to vary the output voltage of the cathode followers by about $\pm$ 0.5v. This adjustment is very fine and stable. Second, as an added convenience, the cathode follower outputs are brought to the ground potential in the absence of signals by suitably choosing the working point.

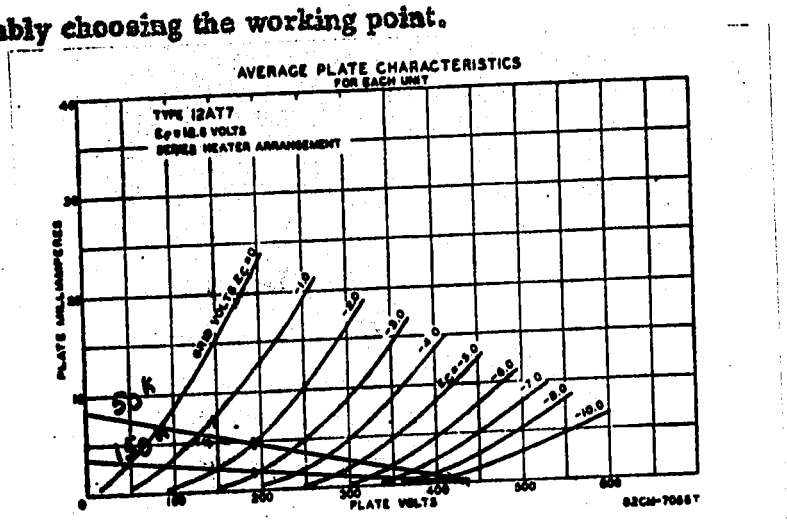

Fig. 2.3-7.

The errors introduced by the presence of the cathode followers are due to the nonlinearities and drift. We have assumed that the cathode follower nonlinearities are negligible.

The drift in the output level is chiefly caused by the supply voltage variations. The filament voltage is maintained constant within 0.01% on the average by an A-C. regulator, and we assume that there is no significant drift due to this cause. Since our specification calls for an output drift not greater than 1μV/sec. therefore, the allowable drift in the plate supply voltage of the cathode followers is

$$\Delta e_b = \Delta e_k \frac{r_p + (1+\mu)R_k}{R_k} = \Delta e_k \mu \qquad (2.3\text{-}6)$$

which for $R_k > r_p$ and $\mu \gg 1$ is very nearly equal to $\Delta e_k \mu$ values of $14.5 \leq r_p \leq 30$, $37 \leq \mu \leq 57$ the admissible plate supply drift becomes about 50μV/sec.

This figure will be required in the consideration of the power supplies.

There are two more causes of inaccuracies, both due to the adjustability of the value of the cathode resistance for output level control (elimination of "A" term from the output of the multiplier). These causes are the variations in the gain and output impedance of the cathode followers.

The gain of the cathode follower is given by

$$K = \frac{\mu R_k}{r_p + R_k (1+\mu)} \qquad (2.3\text{-}7)$$

For $14.5 \leq r_p \leq 30$, $37 \leq \mu \leq 57$, and $50k\Omega \leq R_k \leq 150k\Omega$, we obtain $0.979 \leq k \leq 0.98$, this variation in gain results in an error of less than 0.1% and therefore can be neglected.

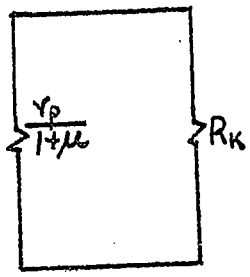

Fig. 2.3-8

The output impedance (see Fig. 2.3-8) for the same assumed values of r_p, μ, R_k, we have $300 \leq Z_{out} \leq 800\Omega$ which imposes the conditions on the input resistance of the integrators.

To make the errors due to the output impedance changes less than 1% the integrators should have an input resistance not less than 50kΩ.

Integrators

The noise measuring technique used in this project is based on the fact that if two uncorrelated random signals of zero mean value are multiplied together, their product is zero on the average. This implies that the output of the multiplier (Equation 2.3-2) has to be averaged in time.

$$\lim_{T\to\infty} \frac{1}{T}\int_0^T (x^2+xz+xy+yz)dt = \overline{x^2} \quad \text{(see section 2.1).}$$

This averaging can be done by an integrator. Ideally, the averaging should be extended over an infinite time. Practically a finite average period can be used depending on the required accuracy of the final result.

In the case of noise measurements within a narrow, rectangular shape, bandwidth B and uniform spectral intensity within this bandwidth an integration time T will measure with a relative error of a single measurement β (Burgess 1951).

$$\beta = (2BT)^{-\frac{1}{2}} \qquad (2.3\text{-}8)$$

For f_c = 6Kc and $\beta = 5 \times 10^{-3}$ (0.5%), T should be at least 3 seconds. Therefore, integration times of 10 and 20 seconds were chosen. An additional time constant of 2 seconds was added in order to make adjustment of the multiplier easier

Of the various types of integrators (e.g. simple RC and RL networks, Miller integrator, mechanical integrator (c.f. Pettit, 1959)), we have chosen a simple RC network as the integrator because of its simplicity in designing and operation and, above all, because it can be made to satisfy the specification (c.f. section 2.1). The circuit of RC integrator is shown in Fig. 2.3-9.

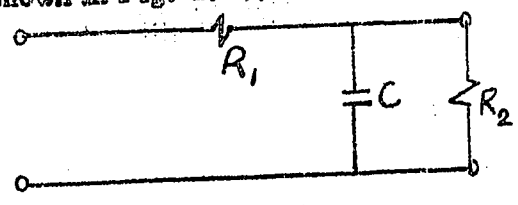

Fig. 2.3-9.

In Fig. 2.3-9, R_2 is made up from the leakage resistance of the capacitor and the input resistance (about 90 MΩ) of the meter.

Integration performed by this integrator is accurate only under certain conditions. These conditions can be inferred from the following argument.

(1) The transfer function H(s) of the circuit of Fig. 2.3-9 is given by

$$H(s) = \frac{R_2}{R_1 R_2 sC + R_1 + R_2} \tag{2.3-9}$$

$$= \frac{\frac{R_2}{R_1 R_2 C}}{\left[s + \frac{R_1 + R_2}{R_1 R_2 C}\right]} \tag{2.3-10}$$

where the operator s is interpreted as the complex frequency

$$s = \sigma + j\omega \tag{2.3-11}$$

under the condition

$$\left| s \right| \gg \frac{R_1 + R_2}{R_1 R_2 C} \tag{2.3-12}$$

Eq. (2.3-12) reduces Eq. (2.3-10) to

$$H(s) \cong \frac{1}{R_1 C s} \tag{2.3-13}$$

which can evidently be treated as an integrator provided there is no initial charge in the capacitor.

For an error not greater than 0.5%, say, $RsC \geq 200$. Since the assumed time constant is 20 seconds, therefore, the frequency at which the integrator will perform satisfactory is $f \geq \frac{200}{2\pi \times 20} = 1.6$ cps. This condition is satisfied in our case since the lowest frequency limit of the amplifier used is about 20 cps.

(2) Since the maximum output impedance of the cathode follower is 800Ω (see output buffer), the input resistance of the integrator should not be less than 50kΩ. The input resistance of this network is essentially that of the resistance R_1 (see Fig. 2.3-9). This imposes the condition that $R \geq 50k\Omega$.

(3) For a time constant of 20 seconds and R = 50kΩ, C is 400 μf. This is a large capacitance and one can expect a fair amount of leakage in it. In addition, there is a leakage due to the input resistance of the meter used for monitoring the output.

Since the combined leakage contributes to the inacurracy of the measurement we have to establish an acceptable upper limit. Assuming that the presence of leakage should introduce not more than 0.2% error we get for the leakage resistance a value of 25 megohms. Since the input resistance of the output meter (Keithley Instruments, Model 150A) is 90 megohm this leaves, as a limit for the capacitor leakage, about 30MΩ.

Since this leakage is not particularly small we have successfully used low voltage tantalex capacitors. (see Appendix 2)

A complete diagram of the integrator used is shown in Figure 2.3-10.

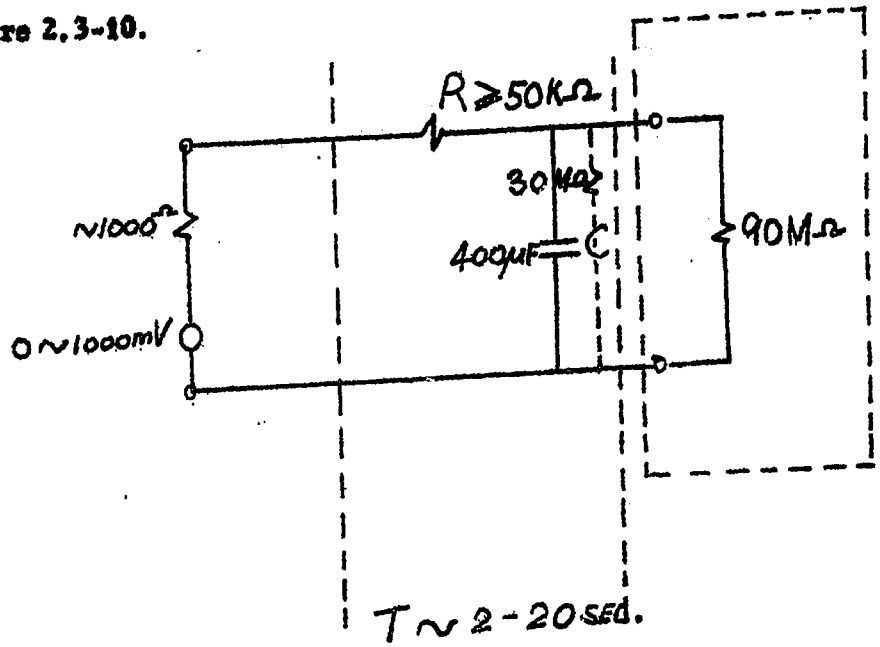

Fig. 2.3-10.

2.4 Measurement of Performance

Error;

The error of the multiplier was estimated to be 1%. The factors contributing to this error are the errors of the input stages 0.2%, the adder 0.4%, the output buffer stage 0.4%, and the non-linear elements 0.5%.

(1) The Buffer stages

Since the main requirements for the buffer stages is the equality of gains for both tubes, the error due to these stages is chiefly due to the unbalance in the gain.

By feeding the same signal of 5 volts peak to peak at 1kc to both tubes and using a cathode ray oscilloscope with a differrential amplifier with 1mv/cm vertical sensitivity as null detector as shown in Fig. (2.4-1a), it was found experimentally that the differential voltage existing between the two Anodes could be reduced to a very small value. The remaining residual voltage, however, due to 120 cps ripple originating from the power supply could not be reduced and was about 2mV. This resulted in a nominal error of buffer gain setting of 0.2%. This ripple could be eliminated by the use of batteries and thus the error due to gain unbalance in this stage could be reduced to a negligible value.

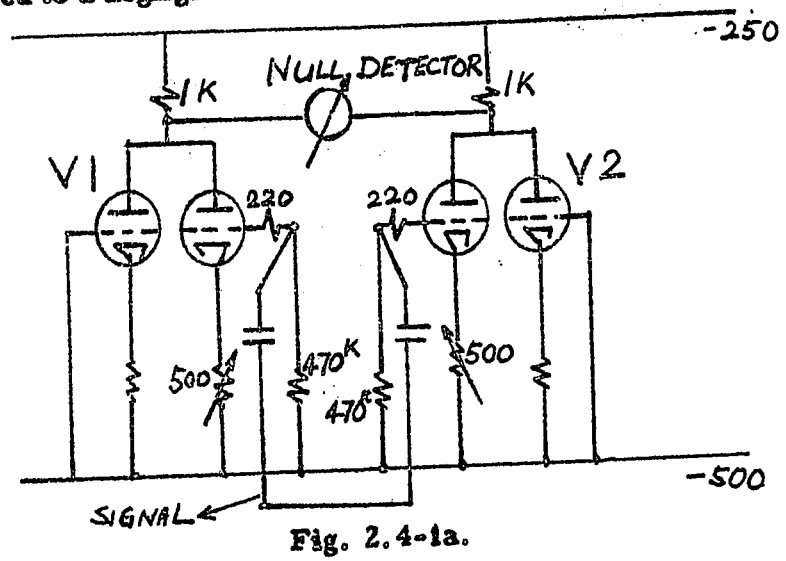

Fig. 2.4-1a.

Variation in gain with respect to output voltage results in non-linearity. According to Valley and Wallman (1948). "The common way of expressing non-linearity is in terms of maximum deviation of the curve of output voltage plotted against input voltage from the best linear approximation thereto, given as a percentage of the total working range of output voltage. This quantity may be related to the change of gain over the length of the curve if the nature of this change is known".

Non-linearity is then expressed as

$$\frac{G_2 - G_1}{G_o} = \frac{\Delta G}{G_o}$$

where ΔG is the difference between the slopes at the extremes of the curve, G_o is the slope of the dashed line, which is the change of gain as a function of input volts over the best fit straight line* gain.

But $$\frac{\Delta G}{G} = \frac{G}{K} \times \frac{\Delta K}{K}$$ (see Appendix 5) (2.4-1)

where $G = \frac{K}{1 - K\beta}$, $1 - K\beta$ is the gain reduction due to negative feedback and K is the gain of the amplifier. The gain of the buffer stage (see section 3) is given by

$$G = \frac{\mu R_L}{r_p + R_k(1+\mu) + R_L}$$

For $30 \leq \mu \leq 60$, $75 \leq r_p \leq 12k\Omega$, $R_L = 1k\Omega$ and $1.6 \leq R_k \leq 1.9k\Omega$.

$0.479 \leq G \leq 0.470$. The difference in gain is only 0.02%.

A geometrical calculation reveals that the non-linearity is

$$\frac{\delta}{V_o} \simeq \frac{1}{10} \frac{\Delta G}{G_o}$$ (2.4-2)

---

* The best-fit-line is meant a straight line AB (refer Fig. 2.4-2) such that the deviations at extreme points A and B and at a point in the middle are the same.

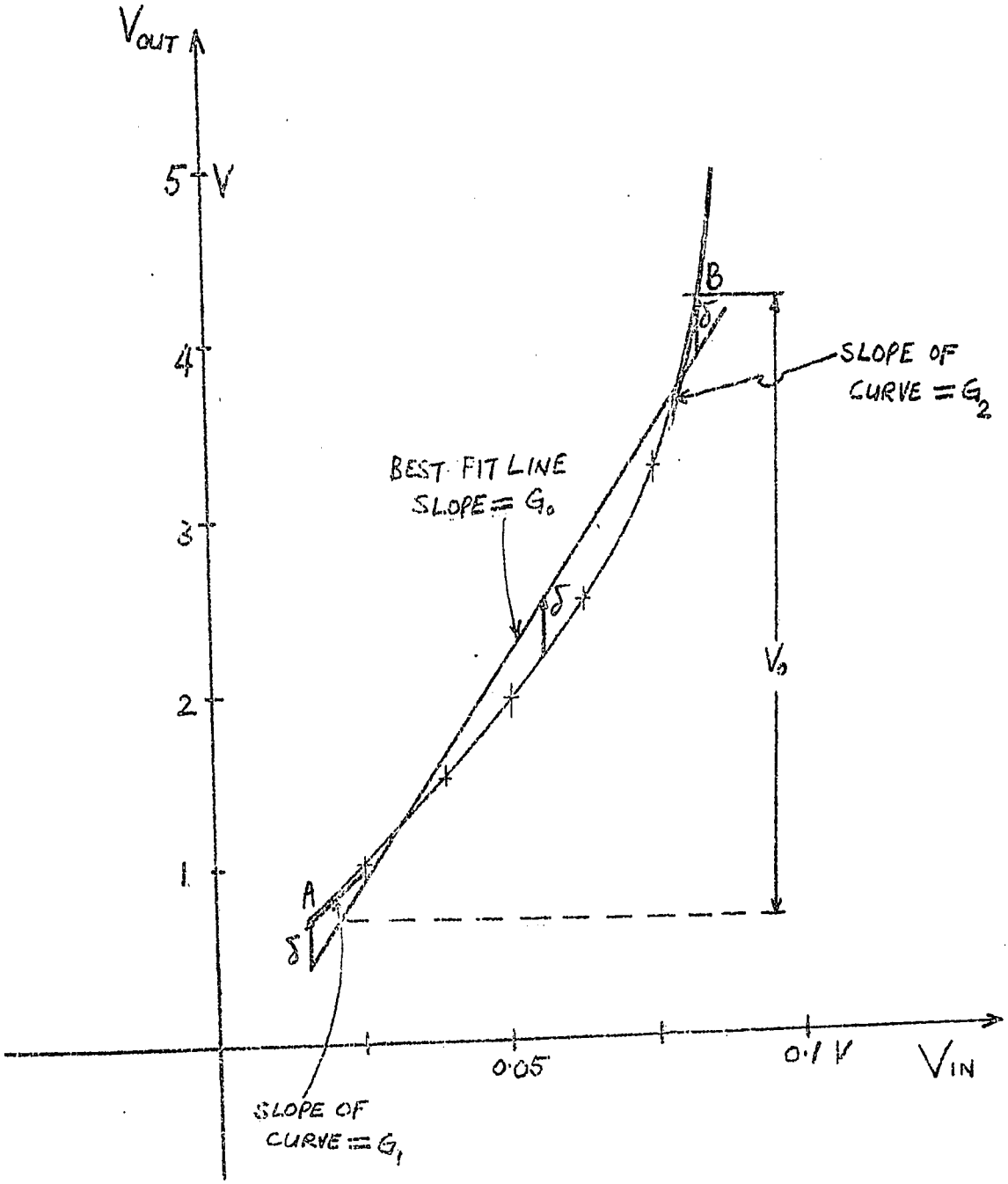
V_{OUT}
5 V
4
3
2
1
B
δ
SLOPE OF CURVE = G_2
BEST FIT LINE SLOPE = G_0
δ
V_0
A
δ
0·05
0·1 V
V_{IN}
SLOPE OF CURVE = G_1

Fig. 2.4-2

where δ is the maximum deviation, V_o is the output voltage. Eqs. (2.4-1) and (2.4-2) show that the fractional non-linearity is decreased by negative feedback in the same ratio as is the gain.

Therefore, as seen from the above discussion, the unavoidable nonlinearity of the tube can be assumed to be negligible because of the large amount of feedback used in the buffer stages.

(2) The adder

The function of these tubes is given in Section 2. Using the same signal and gain of the buffer stages, a similar method for adjusting the gain was used as in (1) but in this case, the null detector was connected as shown in Fig. 2.4-3 and the input to the other half of the adder was grounded.

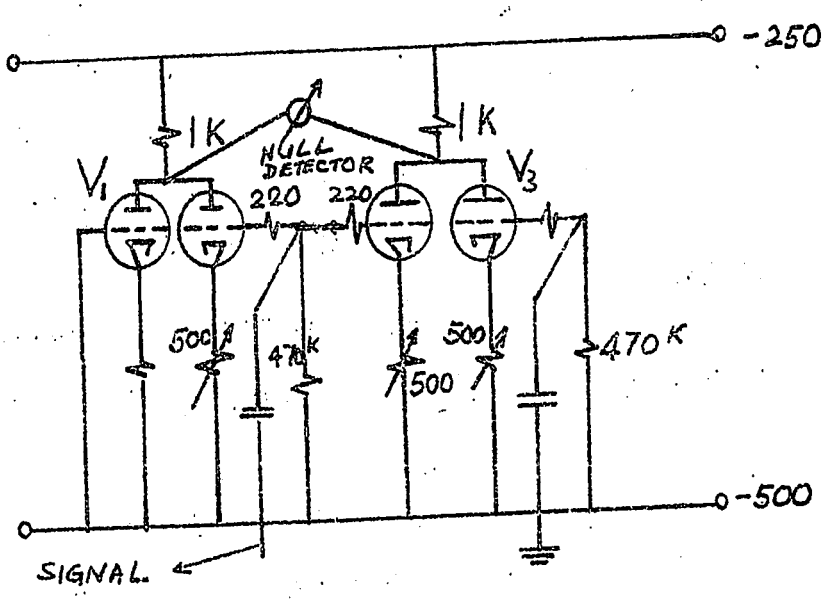

Fig. 2.4-3.

Thus the gain of one of the two adder tubes was adjusted to have the same value as that of the buffer stages.

Since the procedure used here was essentially the same as that used for balancing the buffer stages, therefore, the error was the same as that in (1).

A similar procedure was used for the other tube of the adder.

The overall accuracy of the adder can thus be kept to within $\sqrt{0.2^2 + 0.2^2} \simeq 0.3\%$.

(3) The Output Buffer Stage

The constants A_1 and A_2 (see section 3) of the output of the multiplier can be eliminated by equalizing the outputs in the absence of signals. Using a sensitive DC meter on the scale of 1mV, (Keithley 150A) as a null detector, we could equalize the constants A_1 and A_2 initially to within about 0.1mV. This balance was subject to drift on the order of 2mV/hr.

A similar method for adjusting the gain was used as in (1) and the error was the same as that of (1) but the error due to non-linearity was very much smaller owing to the fact there was much larger amount of feedback in this stage.

By feeding the same signal to both tubes and using a Vacuum Tube Voltmeter (Hewlett Packard Model 400H) as null detector as shown in Fig. 2.4-4, adjusting the variable resistances R_0 and R_1 the output could be balanced to within 0.1 mV on 1mV scale. This balancing was subject to drift on the order of 2mV/hr.

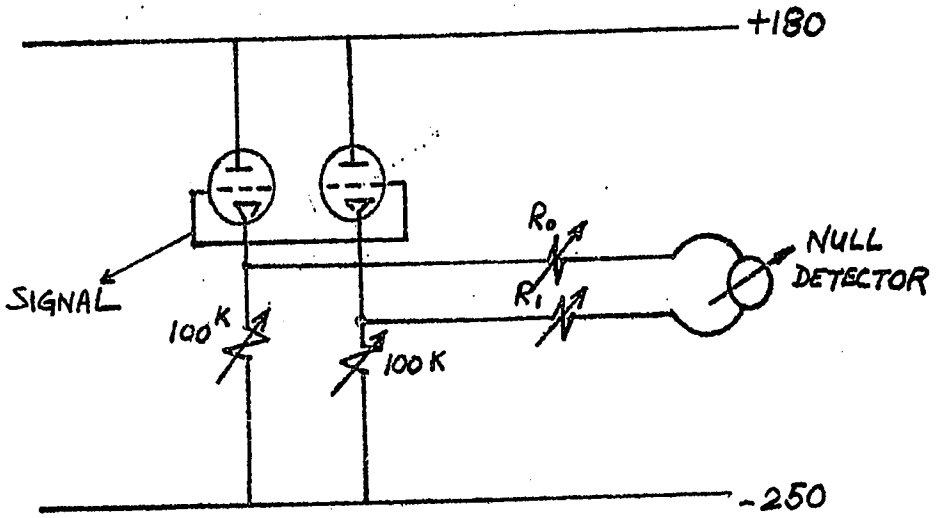

Fig. 2.4-4.

(4) Of all the parts giving rise to errors discussed above, the most critical parts determining the accuracy of this multiplier are the non-linear elements, which we assume to have the current-voltage transfer characteristic of second order (see eq. 2.3.1). If this transfer characteristic is assumed to have a term of the third order then we have

$$I = A + BV + CV^2 + DV^3 \qquad (2.4\text{-}4)$$

the meaning of the symbols being the same as in section 2-2.

The output of the multiplier is then given by $A_3 - (A_1 + A_2)$ $+(B_3 - B_1)X + (B_3 - B_2)y + (C_3 - C_1)X^2 + (C_3 - C_2)y^2 + (D_3 - D_1)X^3$ $+ (D_3 - D_2)y^3 + 2C_3Xy + 3D_3X^2y + 3D_3Xy^2 + B_3y^3$ (2.4-5)

If Y is zero, that is one of the two inputs is grounded, the remaining terms are

$$[A_3 - (A_1 + A_2)] + (B_3 - B_1)X + (C_3 - C_1)X^2 + (D_3 - D_1)X^3 \qquad (2.4\text{-}6)$$

The first three terms are controllable as discussed in section 2, but we have no control over the last term and therefore, the error due to its presence is unavoidable.

To compute numerically the effect of the D coefficient on the multiplier error, two 5670 tubes were tested as described in Appendix 3, and the current-voltage transfer characteristic of these tubes were found to be

$$I_1 = 0.59 + 14.11V + 2.00V^2 + 0.16V^3 \text{ mA} \qquad (2.4\text{-}7)$$

$$I_2 = 0.59 + 14.13V + 4.01V^2 + 0.17V^3 \text{ mA} \qquad (2.4\text{-}8)$$

From equation (2.4-6), it can be seen that the presence of $(D_3 - D_1)$ coefficients give an error of 0.5% (Appendix 3). This error can be further minimized by selecting tubes having D coefficients as nearly equal to one another. This can be easily done by using frequency analyser as described in Appendix 3.

Bandwidth:

The bandwidth of the multiplier was measured by applying a signal to both inputs. The frequency was changed until the output voltage reached 0.707 of its amplitude at mid frequency. The bandwidth found was 1M cycle/sec. (Fig. 2.4-7).

Sensitivity:

To test the sensitivity of the multiplier, a sinusoidal signal of 10kc was applied to each input simultaneously and the output was measured. Fig. 2.4-8 gives the plot of output against the input of the multiplier. From the figure the range of this multiplier was found to be from 600mV - 5V peak to peak.

Drift:

The output of the multiplier was connected to a recorder (Varian Model G-10) and it was found that the drift of the multiplier output is in the vicinity of 10mV in eight hours, as shown in Fig. (2.4-9).

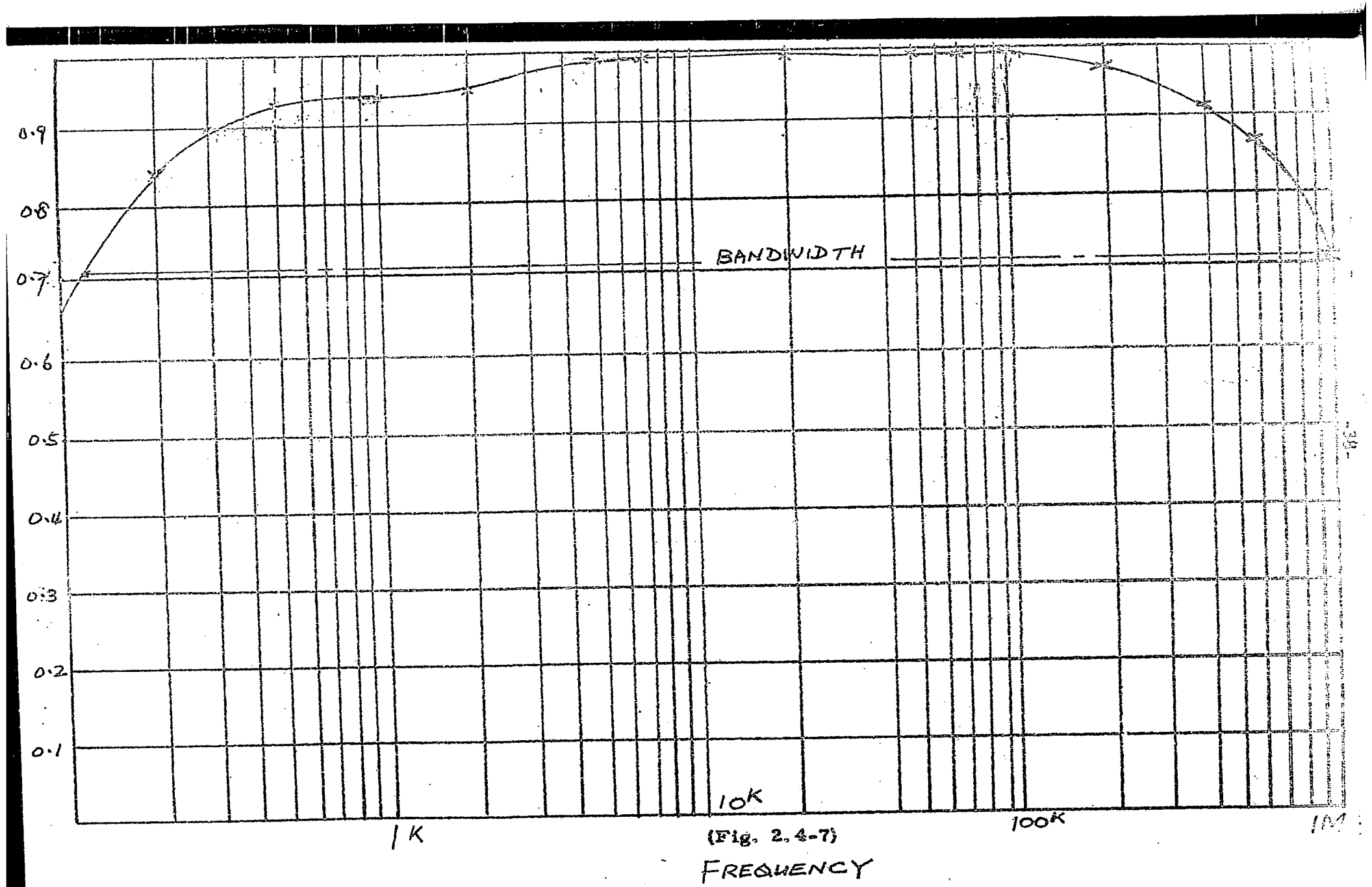

(Fig. 2.4-7)

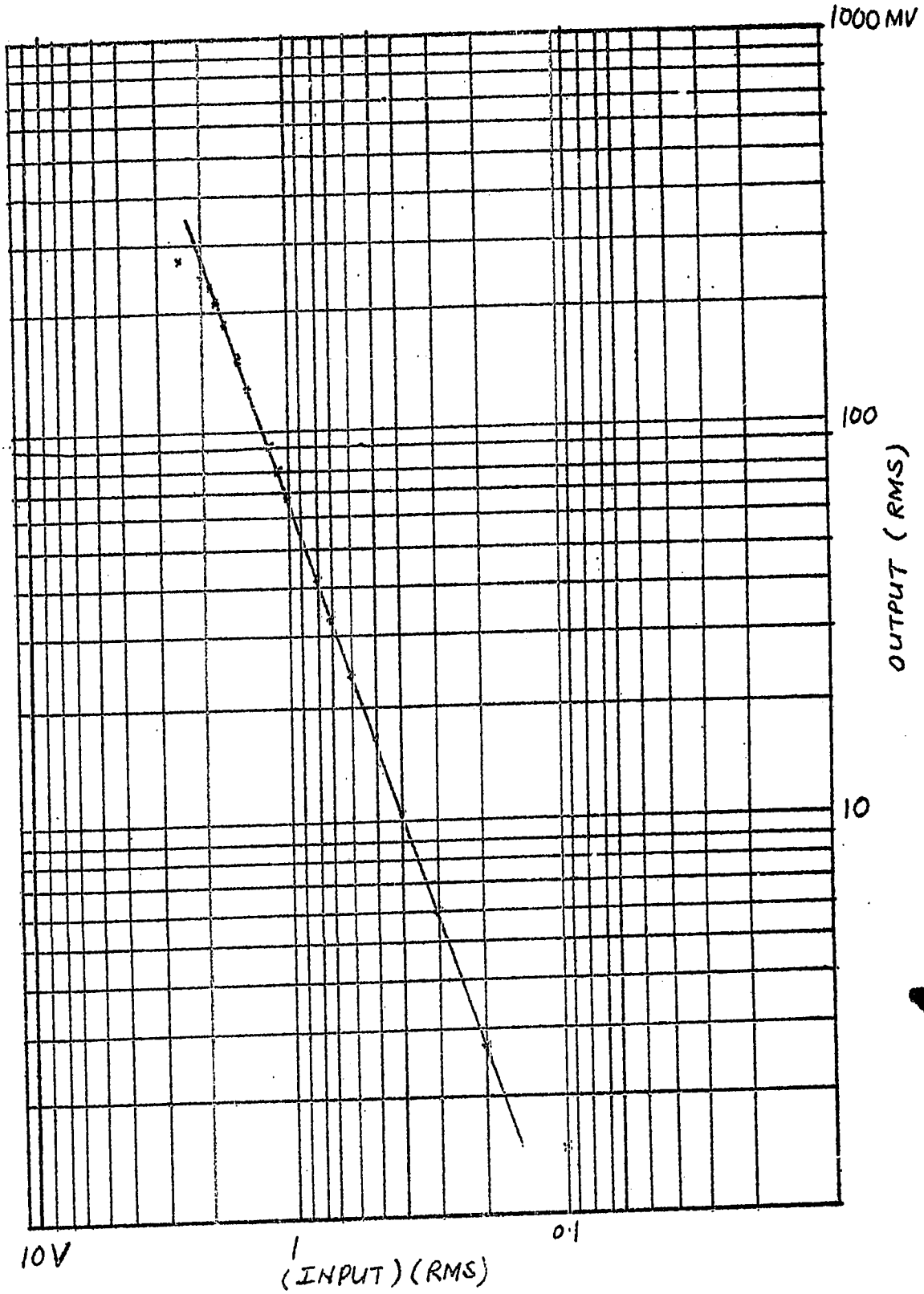

Fig. 2.4-8

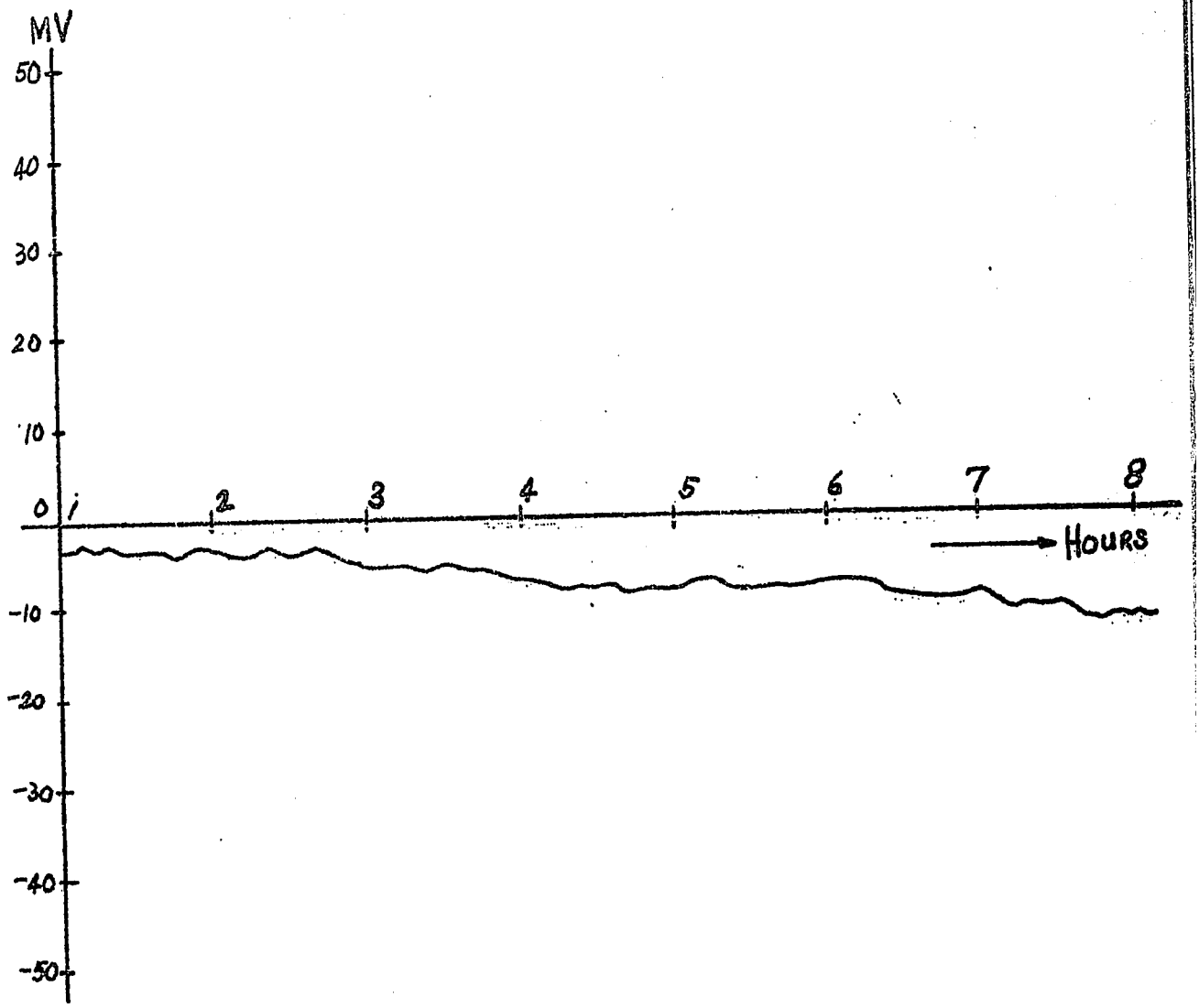

Fig. 2.4-9

A COMPLETE DIAGRAM OF THE

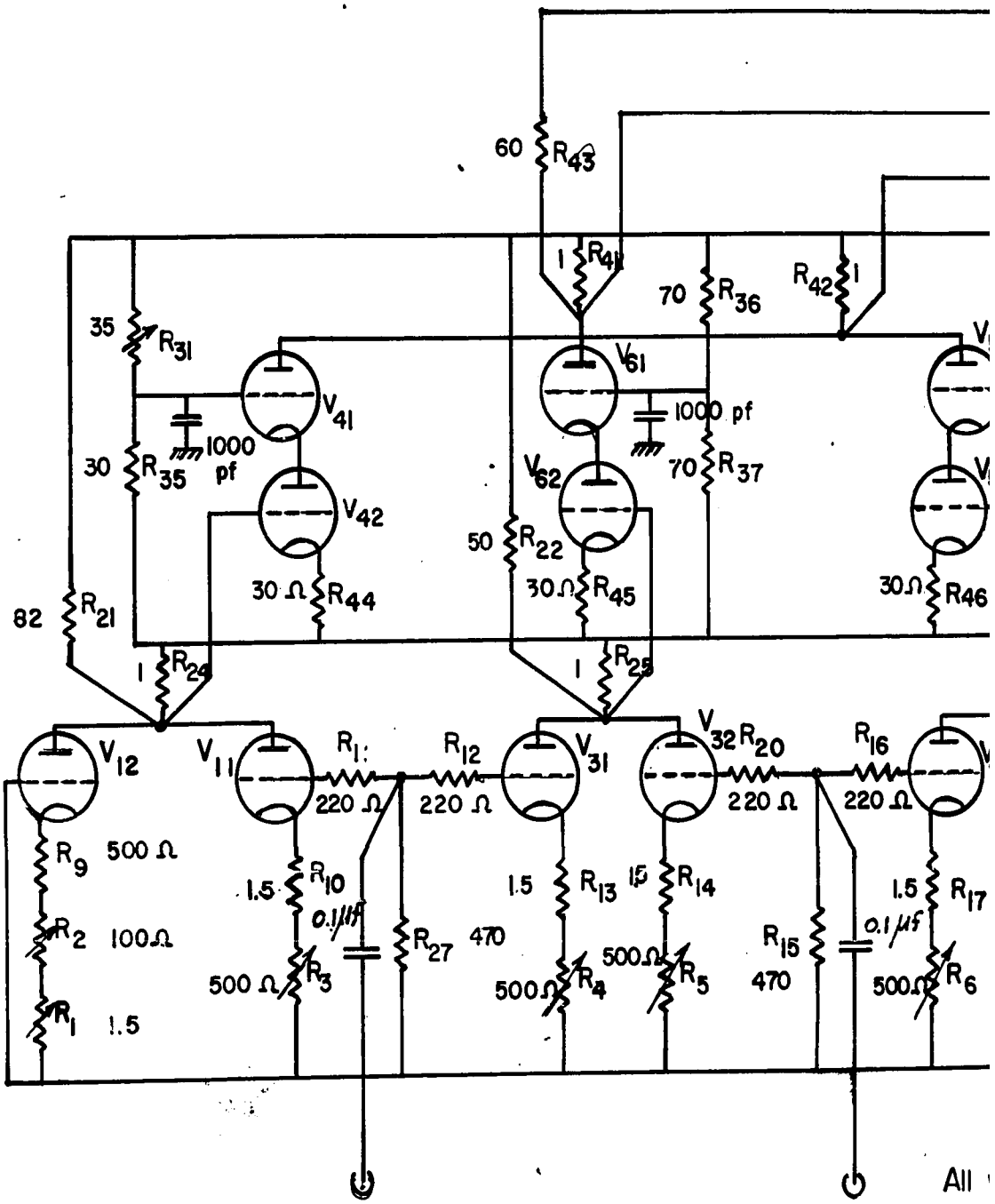

All
othe

Fig. 2.4-10

ETE DIAGRAM OF THE MULTIPLIER

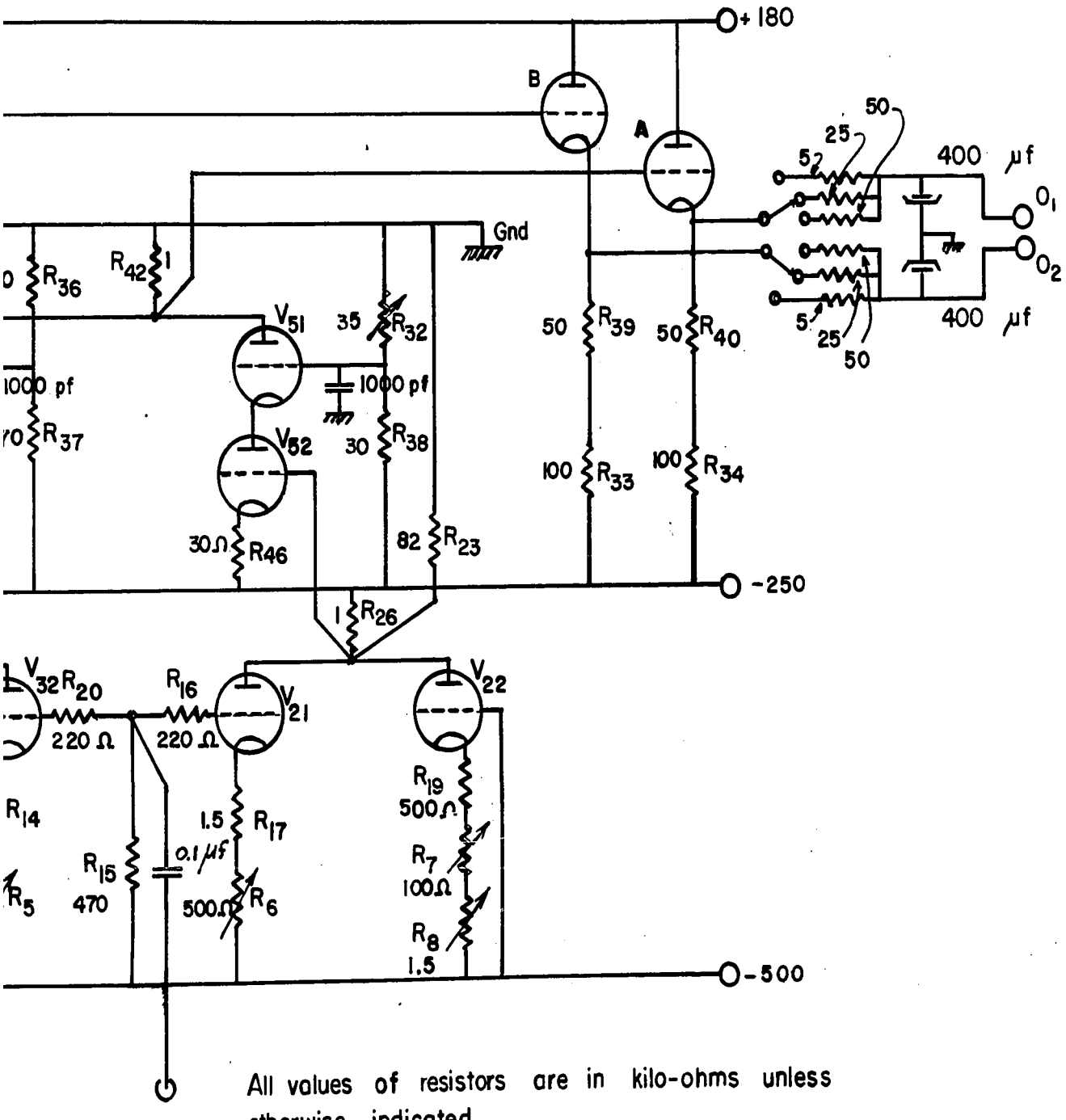

All values of resistors are in kilo-ohms unless otherwise indicated.

CHAPTER 3

Power Supply

The 500 volt supply is used with the positive terminal at ground, and a current of up to about 40mA is drawn at a potential of -500 volts. In addition, a +250 volt terminal is required. Short term stability should be comparable to that of the -500 volt supply. It is suggested that a simple regulator be added, using the 500 volt supply to provide a reference level.

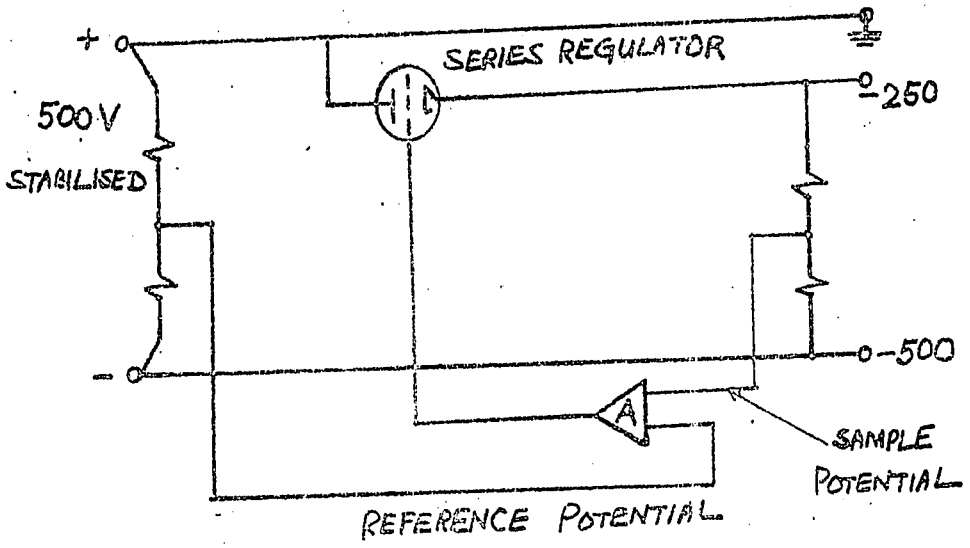

Fig. 3.1

1. Series Regulator :-

The d-c load is relatively light ~50mA - and a receiving type output tube of the 6L6 type is adequate. The voltage drop is fixed (at 250 volts), so the dissipation at 50mA load is only 12.5 watts. The 6L6 WGA is capable of dissipating 17.5 watts and if connected as a triode, has a voltage amplification factor μ of about 8.

2. The Shunt amplifier

(a) D.C. Stability

If we assume that the 500 volt supply has a stability of about 1 in 10^4, our regulator should certainly be as good as this, we might aim at a long term stability of 1 in 10^4, and a short term (minutes) of perhaps ten times better than this.

A balanced double-triode cathode coupled amplifier ("long tail pair") can be relied on to maintain a stable grid-cathode voltage to within 10 millivolts if the heater voltage is stabilized to within about one percent. The variations, ascribed to contact potential changes, would be about $\pm$ 1millivolt over the period of a short term experiment (a few minutes).

If we use a reference voltage, derived from the 500 volt supply, of about one half the final output i.e. 125V then the fluctuation in contact potential would be about doubled when referred to the output terminal. Hence fluctuation due to this cause will be about $\pm$ 20mV in 250V over the long term, and perhaps $\pm$ 2mV over the short term. The stability would only be improved by using an amplifier having less drift --e.g. a chopper-stabilized system. However, $\pm$ 20mV in 250V is a stability of one part in 12,500 which is comparable to the stability of the reference supply and is accepted as adequate.

(b) Amplifier gain --- output Resistance

The output resistance of the stabiliser amplifier, will be approximately that of the follower of the series regulator tube when connected as a cathode follower ($\frac{1}{Gm}$, where gm is the transconductance of the tube) divided by the(voltage) gain around the feedback loop, i.e.

$$Ro \simeq \frac{1}{K} \cdot \frac{1}{Gm} \qquad (3.1)$$

we design the circuit to provide an output resistance which will cause voltage changes due to load current variations to be of similar magnitube as those arising from other causes. Thus if current variations are about $\pm$ 5mA, the terminal voltage variations $\pm\delta V$ will be

$$\delta V = (5\text{mA})R_o \tag{3.2}$$

we should have $\delta V \simeq 2\text{mV}$ (similar to stability fluctuation) which gives $R_o < 0.4$ ohms.

Assuming, for the triode-connected 6L6, that G_m 4,700μmv

$$R_o \leq 0.4 \text{ ohms} \tag{3.3}$$

$$R_o = \frac{1}{K}\,\frac{10^6}{4,700} \text{ ohms}$$

$$K > 530 \tag{3.4}$$

This is the loop gain. The sensing voltage divider will cause a loss of gain of about 2, so that the overall voltage gain must be about 1060 times. The voltage gain includes the μ of the series regulator, which is about 8, so that the actual shunt amplifier should have a voltage gain of 1060÷8 or about 133 times.

(c) Shunt Amplifier-Frequency Response

Because we require one overall phase reversal from input grid to series tube grid, and because long-tail pair amplifier may or may not invert, we have a choice of connection.

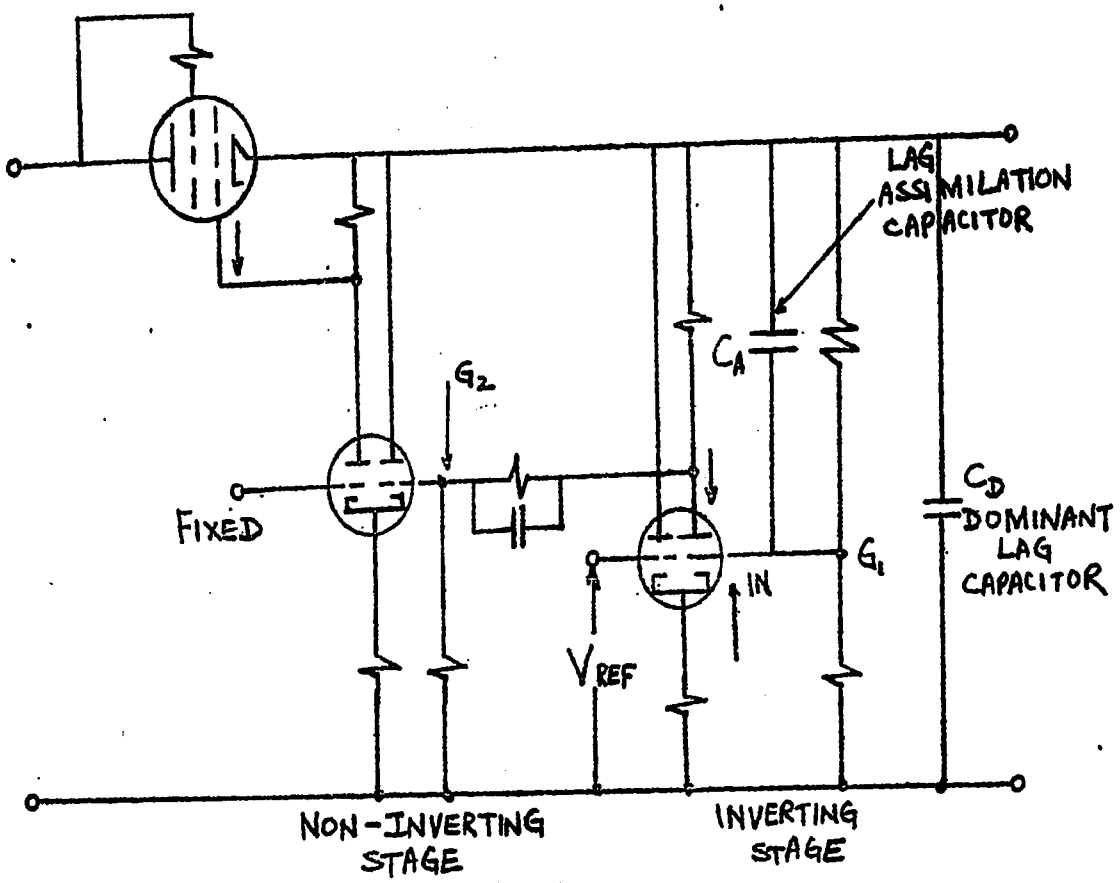

Fig. 3-3

The first stage includes the full complement of Miller effect capacity. The effective input capacitance at point G_1 is

$$\left\{C_{gk} + (1 + K)\, C_{gp}\right\} \qquad (3\text{-}3)$$

where C_{gk} is the capacitance from grid to cathode, C_{gp} the capacitance from plate to grid and K is the gain. For the 12X7, with 100k load, K≅38, $C_{gk} = 1.8\mu\mu F$, $C_{gp} = 1.9\mu\mu F$. C_{in} (1.8 + 39 x 1.9)≅ 76$\mu\mu F$.

The second stage only adds the " cathode follower " contribution. The Miller effect is missing and the total capacitance at G_2 is only 1.8 + 1.9 = 3.7$\mu\mu F$.

3. Phase Lag Analysis:

Stability against Oscillation.

With the arrangement of Fig. 3-3, there are three phase-lags within the feedback loop.

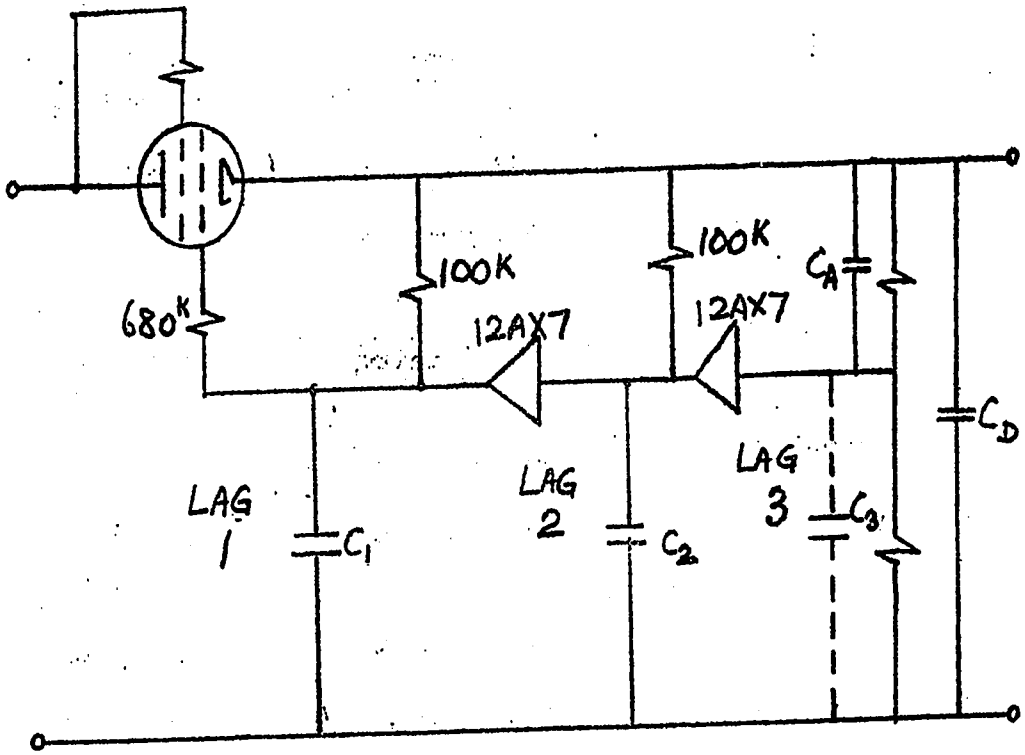

Fig. 3-4

Lag 1.

Capacitance C_1 is made up from:

Input Capacitance, 6L6≃23$\mu\mu$F including strays.

Output Capacitance, 12 AX7≃2$\mu\mu$F.

Total $C_1 \simeq 25\mu\mu F$.

Assume plate load 100k, plate resistor 12 AX7, 80k

Net resistance: 44k = R_1

$C_1 R_1 \simeq 44 \times 10^3 \times 25 \times 10^{-12}$ seconds. (3-4)

$= 1.1 \times 10^{-6}$ seconds.

Lag 2.

Capacitance C_2 is made up from: Input capacitance, 12 AX7, $\simeq C_{gp} + C_{gk} \simeq 4\mu\mu F$, output capacitance, 12 AX7, $\simeq 2\mu\mu F$

say C_2 7.5 F (including 1.5 F for strays)

Net Resistance: 44kΩ R_2. (3-5)

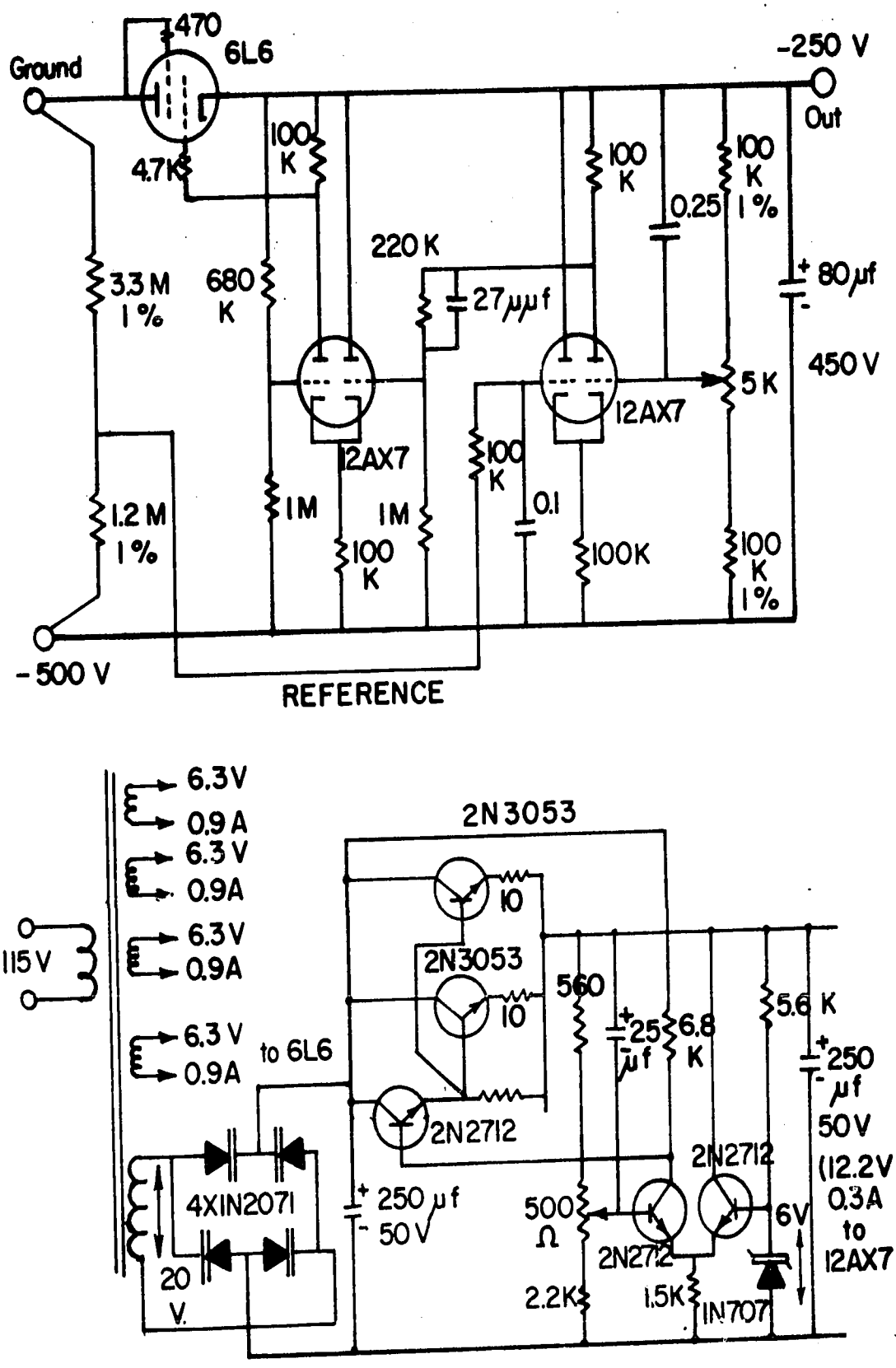
470
6L6
Ground
-250 V
Out
100 K
4.7K
100 K
0.25
100 K 1%
220 K
3.3 M 1%
680 K
27μμf
80μf
450 V
5 K
12AX7
12AX7
100 K
0.1
1.2 M 1%
1M
1M
100 K
100K
100 K 1%
-500 V
REFERENCE
6.3V
0.9 A
6.3 V
0.9A
6.3V
0.9A
6.3 V
0.9A
115 V
2N3053
10
2N3053
10
560
25 μf
6.8 K
5.6 K
250 μf
50 V
to 6L6
2N2712
2N2712
4XIN2071
250 μf
50 V
500 Ω
2N2712
6V
(12.2V 0.3A to 12AX7
20 V.
2.2K
1.5K
IN707

Fig. 3.5

$$C_2 R_2 \approx 0.33 \times 10^{-6} \text{ second.} \qquad (3\text{-}5)$$

Lag 3.

This is made up from the dominant lag capacitor C_D, fed by the generator resistance $\frac{1}{Gm}$ of the 6L6. The largest value of C_D which is reasonable physically is 80 F (450 VDC).

Hence Lag $3 \approx 80$ F $\times \left(\frac{1}{4700} \times 10^{6}\right) \times 10^{-6}$ second. $\approx 1.72 \times 10^{-3}$ seconds.

If we write the time constants as,

$$T_1 = 1.1 \times 10^{-6} = 3.33T$$

$$T_2 = 0.33 \times 10^{-6} = T \qquad (3\text{-}6)$$

$$T_3 = 1.7^2 \times 10^{-3} = 5200\ T$$

Feedback amplifier theory predicts that the overall transfer function develops poles which lie on the jwaxis (axis of real frequency) if:

$$(AB)_{max} = \left(1 + \frac{1}{m}\right)\left(1 + \frac{1}{n}\right)(m + n) \qquad (3\text{-}7)$$

where $m = 3.33$ $n = 5200$

and $(AB)_{max}$ is the critical loop gain. The critical value is thus about 6880. Since we are proposing a lower value of gain (i.e. $\frac{1}{2} \times 38 \times 38 \times 8 \approx 5,800$)

(12 AX7) (12 AX7) (6L6) at the very most we can assume freedom from oscillation. If the gain is reduced to about one quarter of the critical value, the overshoot in response to a step function demand of current will be negligible. This indicates a loop gain of about 1700. The complete regulator is shown in Fig. 3-5, the shunt amplifier heaters are fed with stable d.c. (1%) developed in the conventional transistor regulator. The filament transformer has a number of isolated 6.3 volt windings for feeding the multiplier tubes.

CHAPTER 4

Noise Measurement

The noise measuring apparatus have been assembled as shown in Fig. 4-1.

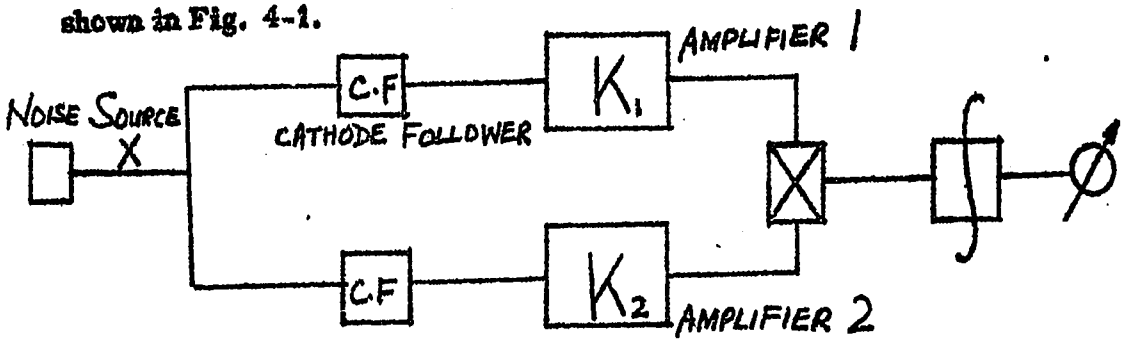

Fig. 4.1.

A cathode follower was installed at the front end of each receiver in order to increase the input impedance which was 200 ohms.

As a starting point each of the amplifiers used here was an RCA Communication Receiver (Model 150A), having a full voltage gain of about 10^7, the bandwidth of 6Kc.

The dynamic range of the multiplier was 600 mV to 5V peak to peak and the bandwidth was about 1Mc. A broad bandwidth multiplier was chosen by Rimawi (1963) because he thought that he could make use of the wide band decade amplifiers (Acton Laboratories, Model 500-A) available in the department but soon he found that the amplifiers had been modified. The voltage gain of the multiplier was 68×10^{-2}.

The integrator has three time constants (2, 10 and 20 seconds). The 2 second time constant was used when making routine measurements on the apparatus. For 10 and 20 seconds, please refer to Section on "Integrators" (Chapter 2).

The meter used here was a sensitive DC meter (Keithley 150A) with ranges from $\pm 1\mu V$ to $\pm$ 1V full scale.

4.2 Measurement Procedure:

The measurement was made with the automatic volume control of each of the receivers switched off and the centre frequency was arbitrarily chosen at 1.5 Mc*.

The output of the receivers, which consisted primarily of the background noise was adjusted and kept within the dynamic range of the multiplier. A CRO (cathode ray oscilloscope) and an RMS (root mean square) voltmeter were used for this purpose.

Various integrating time constants were used to see if the background noise were cancelled. By feeding the two inputs of the multiplier with the same receiver, using a time constant of 10 seconds, the magnitude of the background noise was about 6 millivolts. Then with two receivers, the background noise was about 1mV (c.f Fig. 4-2). Knowing that the background noise was not fully cancelled, a time constant of 20 seconds was used and the background noise was then reduced to about 0.3 mV. (c.f. Fig. 4-2). From these results we knew that longer time constant was needed, but if the integrating time constant was too long, the drift of the power supplies would affect the measurement.

The reading on the DC meter did not give direct reading of the noise voltage measured but with certain interpretation as seen below.

$$\text{METER READING} = K_1 K_2 K_3 \overline{X}^2$$

where K_1 is the gain of the first receiver $\simeq 1 \times 10^6$

K_2 the gain of the second receiver $\simeq 4.5 \times 10^5$

and K_3 the gain of the multiplier $= 68 \times 10^{-3}$

---

* When measuring p-n junction noise, it is advisable to have centre frequency greater than 10 kC in order to avoid the flicker noise. (Bennett 1960).

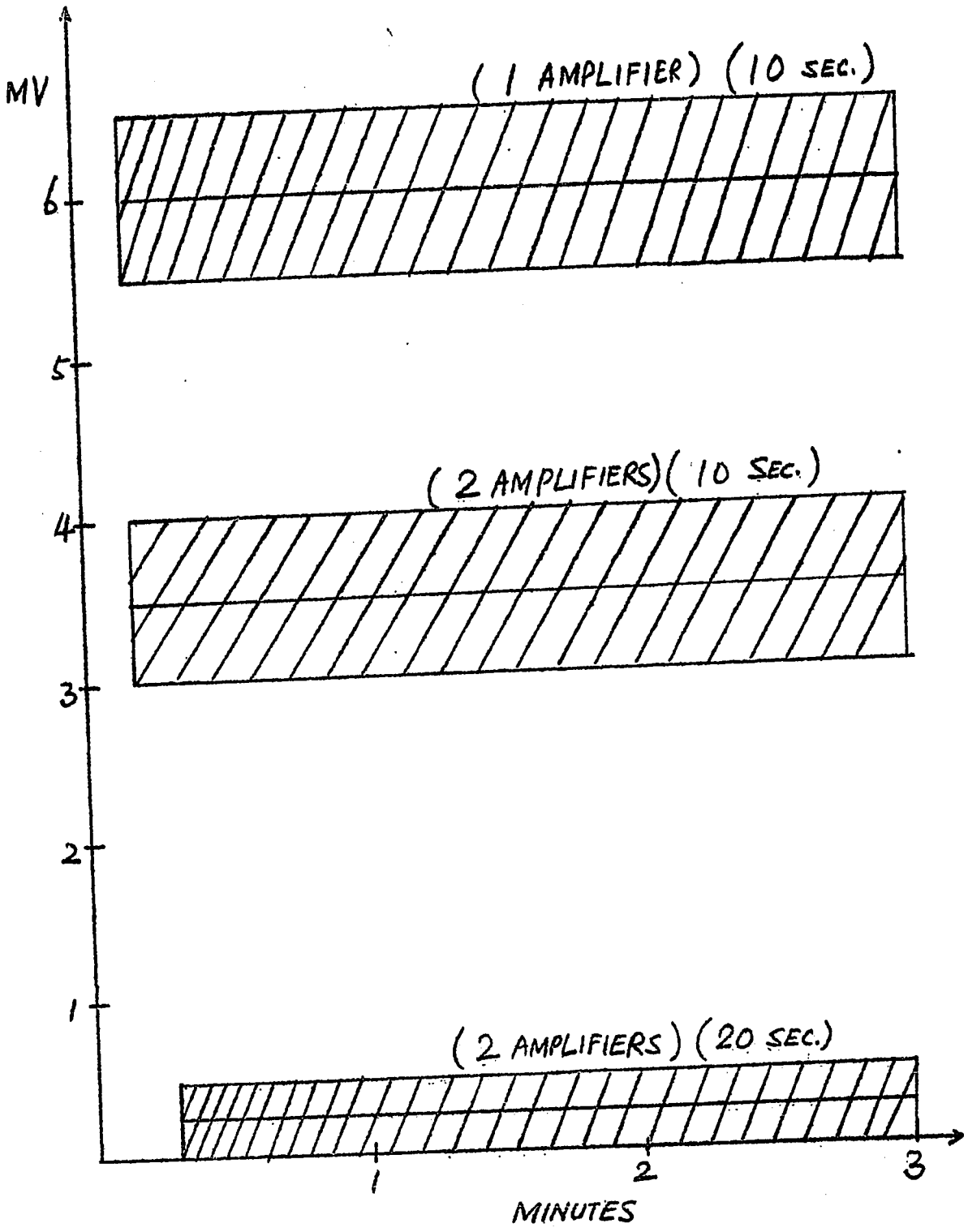
MV
6
5
4
3
2
1
(1 AMPLIFIER) (10 SEC.)
(2 AMPLIFIERS)(10 SEC.)
(2 AMPLIFIERS) (20 SEC.)
1
2
3
MINUTES

Fig. 4-2

The minimum thermal noise originating in resistors that we could measure was kilo-ohm as shown in Fig. 4.3.

Remarks:

When using the apparatus to measure semi-conductor noise, we should use Beat Frequency Oscillator (and detector as mixer) so as to avoid the change of noise spectrum at detection. However, it is not necessary with the white noise i.e. noise originiting within the resistors. It is because when RF stage passes a certain bandwidth $\pm \delta f$ about $f = 1.5$ Mc, the Mixer and IF (Intermediate frequency) filters merely transform all these spectral component to a new centre-frequency and bandwidth. But detector changes the (ideal) rectangular spectrum to a triangular shape due to components beating together in the non-linear detection.

4.3 Proposal for further research:

In order to be able to measure the p-n junction noise biased in the forward direction at high current density, we have to improve the signal to noise ratio. To do this without introducing any significant or comparable noise to the junction noise, a tuned circuit is proposed as shown in Fig. 4.3-1

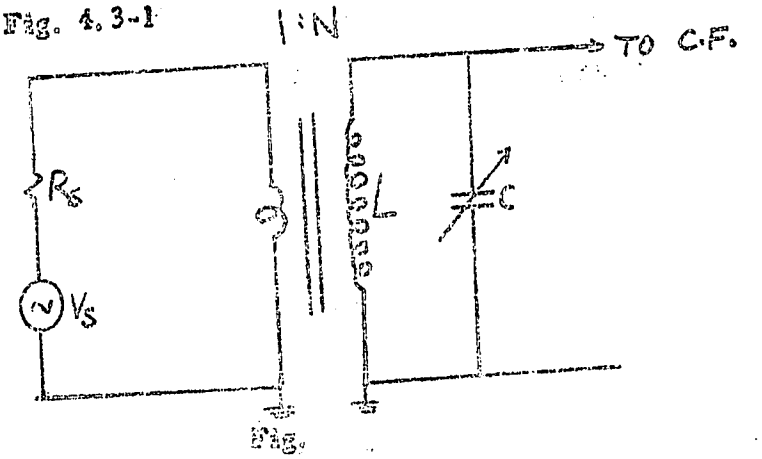

Fig.

This circuit can easily be designed to act as a set-up transformer.

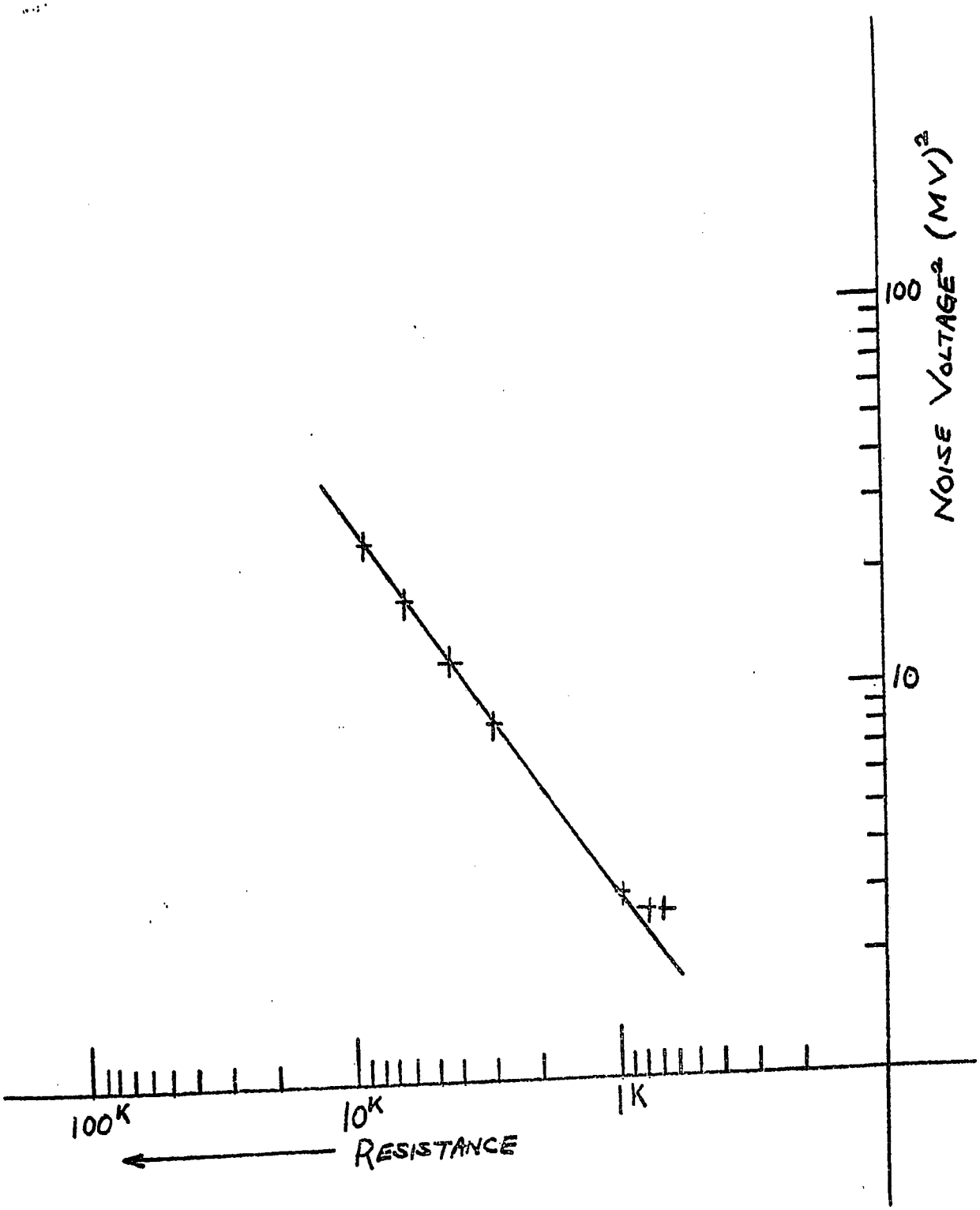

Fig. 4-3

The second method is by using two complete systems in tandem as in Fig. 5-2.

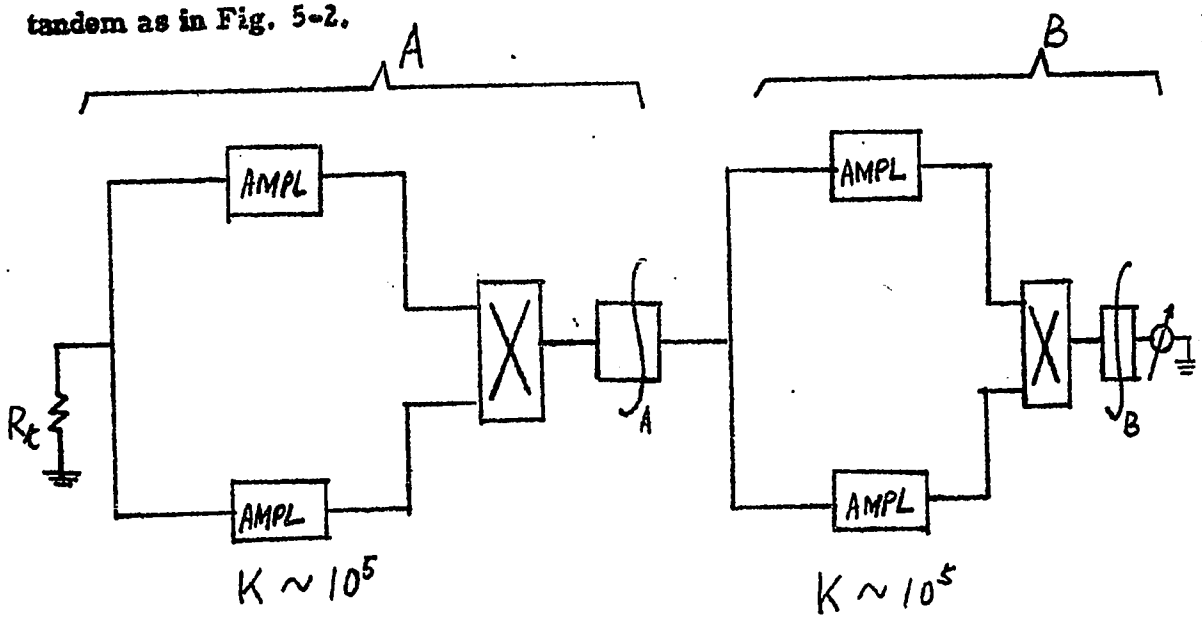

Fig. 5.2.

With such an arrangement it might be possible to increase the total amplification considerably. Since the system B would have to work at frequencies within the passband of the integrator $\int_A$, it would be necessary to use the system A at frequencies high enough to make the passband of $\int_A$ reasonably wide. This condition might not be difficult to realize by working in the VHF or microwave region with the system A.

Conclusion

At the time of starting the work or this project, the most important part of the system was the one described in Chapter 2, the multiplier. Its importance stemmed chiefly from the fact that this was the only part which was required to complete the noise measuring equipment as originally planned in 1961.

As a starting point for the multiplier, an existing design has been adopted (Rimawi 1963). But this multiplier had to be modified so as to make it suitable for the present use. Because of the long integration times ranging from a few seconds to several minutes, the drift of the multiplier output had to be reduced to a minimum. Then this became one of the major tasks in this project. The drift has been reduced from the initial value (at the start of work on multiplier) of a few hundred millivolts per hour to the present figure of about 2 mV per hour. This was achieved by the use of stable components (high stability metal film or wire wound resistors) and the use of stable power supplies (chopper stabilised). John Flunke power supply was used with a specified stability of 0.01% per day and ripple of less than 2 millivolts (RMS).

The accuracy of the multiplier (about 1%), its dynamic range (0.6--5V peak to peak) and bandwidth (about 1 Mc) remained essentially as in the original model of K.D.J. Grosvenor (1959).

The output of a multiplier of this type does not give the product of the input quantities directly. There is a proportionality constant involved such that

$$\text{Output} = K(XY) \qquad \text{(c.f. 2.1-2)}$$

This constant K was found to be 68×10^{-3} for this particular multiplier.

This constant, together with the small range of multiplier input imposed severe limitations on the sensitivity of the noise measurements made with our equipment.

The smallest signal with which the multiplier would produce a measurable output was 600 mV (peak to peak). At the same time the largest acceptable voltage was 5 volts (peak to peak).

The largest voltage was determined by the background noise of the receiver. In order not to exceed 5 volts peak to peak of noise output, the receiver gain had to be kept low (about 10^6). In order to produce the minimum signal acceptable by the multiplier the noise source that we wished to measure had to deliver about $\frac{0.6}{10^6} = 6 \times 10^{-7}$ V peak to peak or 2×10^{-7} V r.m.s. This was equivalent to a thermal noise originating in a resistance of about 1 kilo-ohm. It is therefore impossible to measure the noise of 10^{-8} V r.m.s. from a p-n junction biased in the forward direction unless the multiplier has a wider range so that we could fully use the gain of the receiver (about 10^7) or to improve the signal to noise ratio.

The noise voltage that we could measure are far from what was expected from this equipment and can only be regarded as starting point for further developments.

Two suggestions, either of which may enable the apparatus to be used to measure the noise power in a forward biased p-n junction have been put forward in Section 4.3.

Appendix 1.

Suppose the plate current of a triode is given by

$$i_a = a + bv + cv^2 + dv^3$$

where i_a is the actual plate current, a, b, c and d are constants, and v is the grid signal. Values of i and v are assumed to be given and it is required to give the formula or a curve that gives the best fit (set) of the experimental data. For the best fit, the error due to the fitting must be minimized :

$$e = E(i - i_a)^2$$

where e : error

i : given current

E : The mathematical expectation (or average) of the quantity involved.

Expanding the right-hand side,

$$e = E(i^2 - 2ii_a + i_a^2) = E[i^2 - 2i(a + bv + cv^2 + dv^3) + (a + bv + cv^2 + dv^3)^2]$$

To minimize the error ' e ', its partial derivatives with respect to a, b, c and d should be zero. The conditions obtained from such differentiation are the following,

$$\frac{\delta e}{\delta a} = E[-2i + 2(a + bv + cv^2 + dv^3)]$$

$$= -E(2i) + E(2a) + E[2(bv + cv^2 + dv^3)] = 0 \qquad (1)$$

$$\frac{\delta e}{\delta b} = -E(2iv) + E(2bv^2) + E[2v(a + cv^2 + dv^3)] = 0 \qquad (2)$$

$$\frac{\delta e}{\delta c} = -E(2iv^2) + E(2cv^4) + E\left[2v^2(a+bv+dv^3)\right] = 0 \qquad (3)$$

$$\frac{\delta e}{\delta d} = -E(2iv^3) + E(2dv^6) + E\left[2v^3(a+bv+cv^2)\right] = 0 \qquad (4)$$

The constants a, b, c and d are found by solving the equations 1, 2, 3 and 4 simultaneously. The constants are given by the following relations:

$$a\,E(1) + bE(v) + cE(v^2) + dE(v^3) = E(i)$$

$$a\,E(v) + bE(v^2) + cE(v^3) + dE(v^4) = E(iv)$$

$$a\,E(v^2) + bE(v^3) + cE(v^4) + dE(v^5) = E(iv^2)$$

$$a\,E(v^3) + bE(v^4) + cE(v^5) + dE(v^6) = E(iv^3)$$

$$a = \frac{\begin{vmatrix} E(i) & E(v) & E(v^2) & E(v^3) \\ E(iv) & E(v^2) & E(v^3) & E(v^4) \\ E(iv^2) & E(v^3) & E(v^4) & E(v^5) \\ E(iv^3) & E(v^4) & E(v^5) & E(v^6) \end{vmatrix}}{\Delta}$$

$$b = \frac{\begin{vmatrix} E(1) & E(i) & E(v^2) & E(v^3) \\ E(v) & E(iv) & E(v^3) & E(v^4) \\ E(v^2) & E(iv^2) & E(v^4) & E(v^5) \\ E(v^3) & E(iv^3) & E(v^5) & E(v^6) \end{vmatrix}}{\Delta}$$

$$c = \frac{\begin{vmatrix} E(1) & E(v) & E(i) & E(v^3) \\ E(v) & E(v^2) & E(iv) & E(v^4) \\ E(v^2) & E(v^3) & E(iv^2) & E(v^5) \\ E(v^3) & E(v^4) & E(iv^3) & E(v^6) \end{vmatrix}}{\Delta}$$

$$d = \frac{\begin{vmatrix} E(1) & E(v) & E(v^2) & E(i) \\ E(v) & E(v^2) & E(v^3) & E(iv) \\ E(v^2) & E(v^3) & E(v^4) & E(iv^2) \\ E(v^3) & E(v^4) & E(v^5) & E(iv^3) \end{vmatrix}}{\Delta}$$

where $\Delta = \begin{vmatrix} E(1) & E(v) & E(v^2) & E(v^3) \\ E(v) & E(v^2) & E(v^3) & E(v^4) \\ E(v^2) & E(v^3) & E(v^4) & E(v^5) \\ E(v^3) & E(v^4) & E(v^5) & E(v^6) \end{vmatrix}$

Appendix 2.

A comparison between the electrolytic and tantalex capacitors is shown in Fig. A.2-1

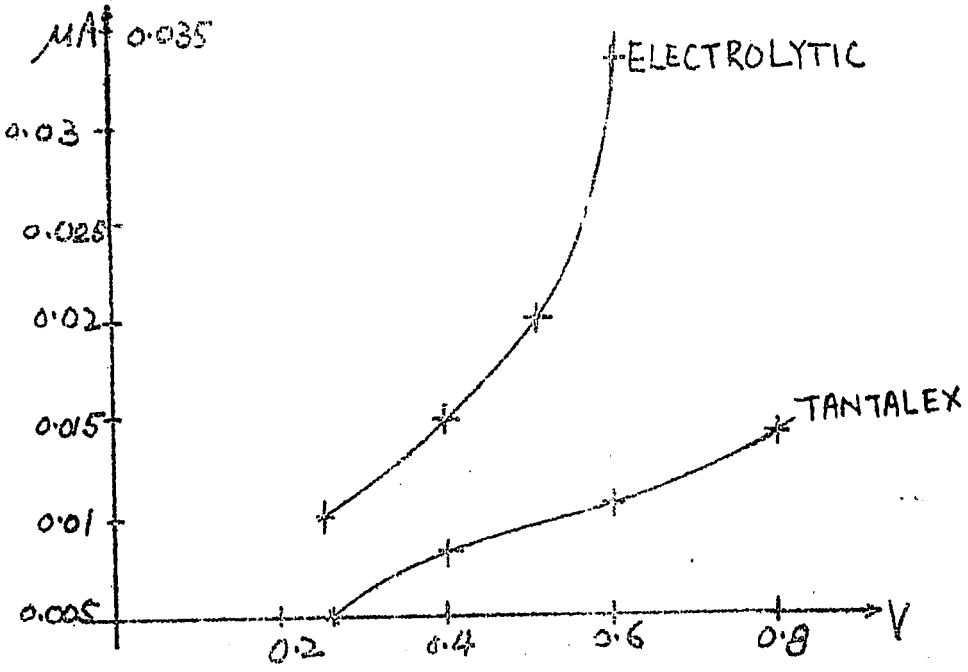

Fig. A.2-1

The above curves were obtained from Fig. A.2-2.

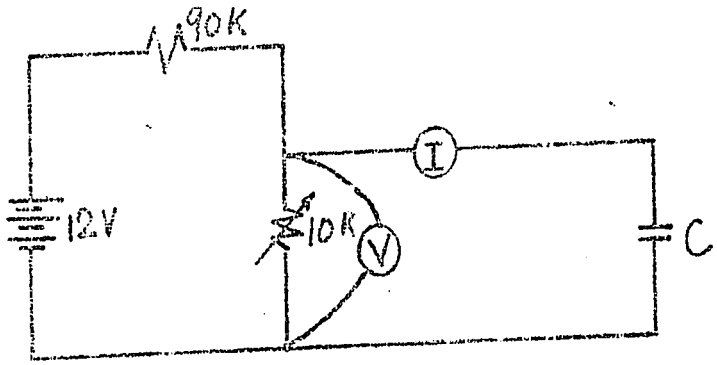

Fig. A.2-2.

It can be seen that over the range of voltage from about 0.2 to 0.6 volts, the leakage resistance of the Tantalex capacitor is nearly constant, being about 60 Megaohms ± 6 Megaohms. Comparable figures for the electrolytic capacitor are 24 Megaohms ± 6 Megaohms.

Appendix 3

If we assume that the non-linear elements have the current voltage transfer characteristic of the third order, then

$$I = A + BV + CV^2 + DV^3$$

where A, B, C and D are constants, and V is the signal voltage.

Applying a sinusoidal voltage of 1 volt peak to peak biasing at -2.5V, by using the frequency analyser (Bruel and Kjaer Type 2105), the constants are found to be

$A_1 = 0.59$	$A_3 = 0.59$
$B_1 = 14.11$	$B_3 = 14.13$
$C_1 = 2.00$	$C_3 = 4.01$
$D_1 = 0.16$	$D_3 = 0.17.$

From Eq. 2.4-6, we see that the $(D_3 - D_1)$ term contributes an error of

$$\frac{(D_3 - D_1)}{C_3 - C_1} \times 100\% = 0.5\%.$$

If this transfer characteristic has terms higher than the third order, the frequency analyser is unable to measure that constant (say E) because it is very small.

Appendix 4

Selection of Tubes in Cascode stages.

It has already been said that the coefficients in Eq. (2.3-1) can be adjusted. However, such adjustment is only practicable if the tubes are initially well matched. Some selection is therefore necessary.

The absolute value of the plate current at the working point is not important (c.f. Section 2.3) but the absolute value of G_m is. In the tubes used, the values of G_m in the centre of the linear portion of $G_m(v)$ curve should be as close to each other as possible (within 5%, say.) At the same time, the slopes of these curves should also be as close to each other as possible (within 20%, say).

The pre-selection of the tubes is carried out in the Vacuum Tube Bridge (GRC No. 561 - D). Each tube has been measured under working condition as in the cascode configuration and the circuit is shown in Fig. 2.4-10.

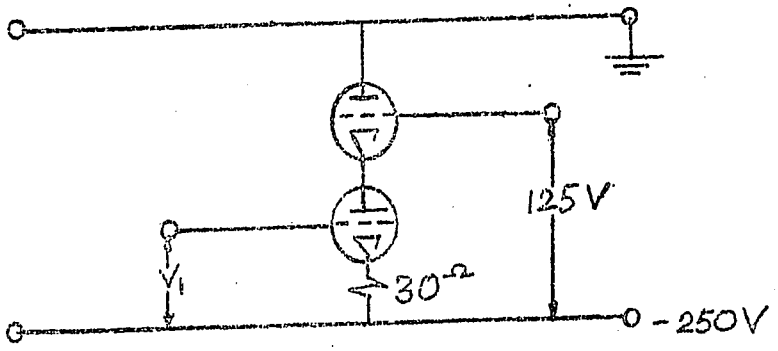

Fig. 2.4-10.

Typical results for the measurements are shown in Fig. 2.4-11. Curves (1) and (3) have nearly the same slope of G_m but the linear portion is too far apart. Curve (2) is not as linear as that of curves (1) and (3) although it stays within the superposition limit (5%). From experience, we can choose any curves for our reference and try to pick as similar tube characteristic as possible from the experimental results.

Good selection of the tubes will give a wider range of multiplication, thus obtaining a better multiplier because of the identical G_m ("b" constant) and slope of G_m ("c" constant) (c.f. eq. 2.2-3)

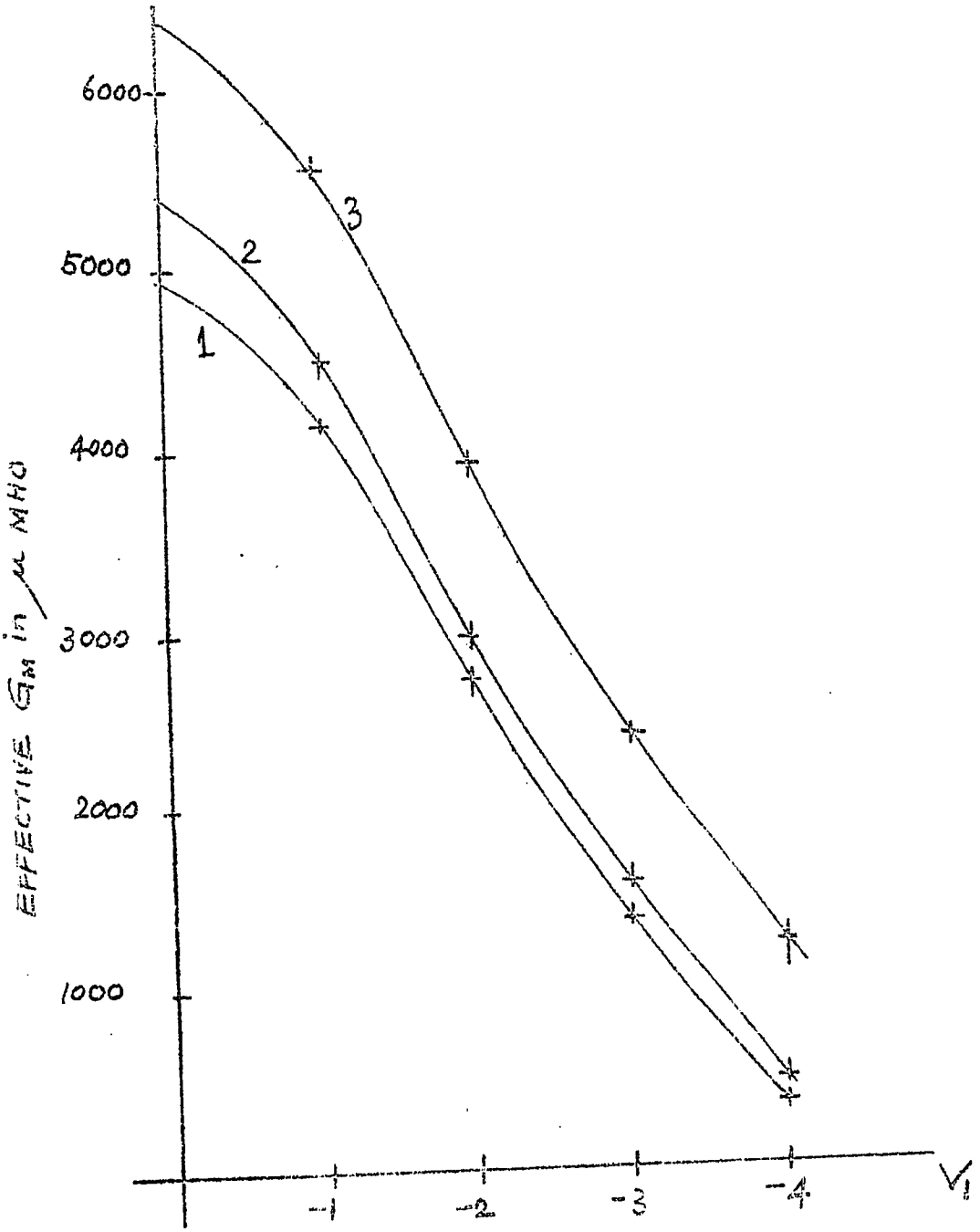

Fig. 2.4-11

Appendix 5.

The common form of the feedback equation is

$$G = \frac{k}{1 - k\beta} \qquad \text{(A.5-1)}$$

where k is the gain without feedback, G is gain with feedback and β is the fraction of output voltage that is added to the input voltage.

If β is kept constant in eq. (A.5-1)

$$\Delta G = \frac{\Delta k(1 - k\beta) - k(-\beta \Delta k)}{(1 - k\beta)^2}$$

$$= \frac{\Delta k}{(1 - k\beta)^2} = \frac{G}{k} \frac{\Delta k}{(1 - k\beta)} \qquad \text{(A.5-2)}$$

$$\Delta G = \frac{G^2 \Delta k}{k^2} \qquad \text{(A.5-3)}$$

or $$\frac{\Delta G}{G} = \frac{G}{k} \cdot \frac{\Delta k}{k} \qquad \text{(A.5-4)}$$

Appendix 6.

A. van der Ziel expects a considerable space charge outside the junction causing a correlation between carriers thus violating one of the assumptions on which Eq. (1.1-9) is based (independent crossings of the junction by carriers). W. Guggenbuehl and M.J.O. Strutt, on the other hand, expect that the number of carriers drawn into the junction might be influenced by voltage variations, which are caused by variations of the carrier concentration outside the junction.

BIBLIOGRAPHY

1. Fletcher, N. H., 1957, Proc. Institute Radio Engineers N. Y. 45, 862.

2. Gribnikov, Z. S. and Tolpygo, K. B., 1957, Zh. Tech. Fiz. 27, 625.

3. Freeman, J. J., "Principles of Noise," John Wiley and Son, New York.

4. Herlet, A., 1956, F. Naturfg., 11a, 498.

5. Kosenko, 1957, Zh. Tech Fiz 27, 452.

6. Shockley, W., 1949, Bell System Tech. J., 28, 435.

7. Tolpygo K. B., 1956 Zh. Tech. Fiz. 26, 293.

8. Tolpygo K. B., and Zaslavskaya, I. G. 1955 Zh. Tech. Fiz. 25, 955.

9. G. M. Avak'yants, V. I. Murgyin, L. S. Sauder et al, "Forward properties of a p-n junction at high current densities." (Oct 1963, 167)

10. G. M Avak'yants V. I. Murgyin, A. D. Ozheredov and A. Teshabayev: (Sept. 1963, 1521).

11. N. P. Yesina, N. V. Zotova and D. N. Nasledov: (Sept. 1963, 1529).

12. Eberhard Spenke "Electronic Semiconductors."

13. A. Van der Ziel, "Fluctuation Phenomena in Semi-conductors" (1959)

14. B. Schneider and G. J. O. Strutt; "Shot and Thermal noise in Germanium and Silicon Transistor at High Level Current Injections" Proc. IRE; 48; 1731-1739 Oct. 1960.

15. A. Van der Ziel, "Noise in Junction Transistors" Proc. IRE; 46; 1019-1038; June 1958.

16. W. Guggenbuehl and M. J. O. Strutt; "Theory and Experiment on Shot Noise in Semiconductor Junction Diodes and Transistors," Proc. IRE; 45; 839-854; May 1957.

17. H. F. Matari, "Theory on Diode and Transistor Noise" Proc. IRE. 46, 1964; Dec. 1958.

18. E. R. Chenette and A. Van der Ziel. "Accurate noise measurements on Transistors" IRE Tran. on Electron Devices. 123-126, March 1962.

BIBLIOGRAPHY

1. Fletcher, N.H., 1957, Proc. Institute Radio Engineers N.Y. 45, 862.
2. Gribnikov, Z; S. and Tolpygo, K.B., 1957, Zh. Tech. Fiz. 27, 625.
3. Freeman, J.J., "Principles of Noise," John Wiley and Son, New York.
4. Herlet, A., 1956, F. Naturfg., 11a, 498.
5. Kosenko, 1957, Zh. Tech Fiz 27, 452.
6. Shockley, W., 1949, Bell System Tech. J., 28, 435.
7. Tolpygo K.B., 1956 Zh. Tech. Fiz. 26, 293.
8. Tolpygo K.B., and Zashavshaya, I.G. 1955 Zh. Tech. Fiz. 25, 955.
9. G.M. Avak'yants, V.I. Murgyin, L.S. Sander et al,"Forward properties of a p-n junction at high current densities." (Oct 1963, 167')
10. G.M Avak'yants V.I. Murgyin, A.D. Ozheredov and A. Teshabayev: (Sept. 1963, 1521).
11. N.P. Yesina, N.V. Zotova and D.N. Nasledov: (Sept. 1963, 1529).
12. Eberhard Spenke"Electronic Semiconductors."
13. A. Van der Ziel, "Fluctuation Phenomena in Semi-conductors." (1959)
14. B. Schneider and G.J.O. Strutt; "Shot and Thermal noise in Germanium and Silicon Transistor at High Level Current Injections" Proc. IRE; 48; 1731-1739 Oct. 1960.
15. A. Van der Ziel, "Noise in Junction Transistors" Proc. IRE; 46; 1019-1038, June 1958.
16. W. Guggenbuehl and M.J.O. Strutt; "Theory and Experiment on Shot Noise in Semiconductor Junction Diodes and Transistors," Proc. IRE; 45; 839-854; May 1957.
17. H.F. Matari, "Theory of Diode and Transistor Noise" Proc. IRE. 46, 1964; Dec. 1958.
18. E.R. Chenette and A. Van der Ziel, "Accurate noise measurements on Transistors" IRE Tran. on Electron Devices, 123-126, March 1962.

19. W.C. Brunche, E.R. Chenette, and A. Van der Fiel, IRE Trans. Electrons Devices, Feb. 1964.

20. Pettit, Electronic Switching, Timing, and Pulse circuits 1961.

21. L.C. Oakley, Electronic. Industr. (U.S.A.) Vol. 21, No. 10. 145-7 (Oct. 1962)

22. J.P. Holland, "Stabilised High Voltage Supplies". Industr. Electronics. (G.B) Vol. 1, No. 11, 595-7 (Aug. 1963).

23. A. Santel, Onde Elect. (France) Vol. 43. 570-9 (May 1963).

24. W.R. Samarob, "Temperature Dependence of Noise in P-N Junctions" (1961). M.Sc. Thesis, Electrical Engineering Dept., Uni. of Ottawa.

25. J. H. Rimawi, "A Square-Law Multiplier" (1963) M.Sc. Thesis, Electrical Eng. Dept., Uni. of Ottawa.

26. K.D.J. Grosvenor, "A single-quadrant, Video Frequency Electronic Multiplier" (1959).

VITA

NAME: Teong-Cheng Lim

BORN: Penang, Malaya, Oct 4, 1939

EDUCATED:

PRIMARY: Chung Ling High School, Penang, Malaya

SECONDARY: Chung Ling High School, Penang, Malaya

UNIVERSITY: National Taiwan University Taipei, Taiwan, Formosa

COURSE: Electrical Engineering (Communication)

DEGREE: B.Sc. (Electrical)